People`s Democratic Republic of Algeria

Ministry of Higher Education and Scientific Research

University of Echahid Hamma Lakhdar - El Oued

ACADEMIC MASTER

Domain: Science and Technology

Division: Electrical Engineerimg

Specialty: Electrical Control

Presented by:

Ben Haoua Salman

Entitled:

Robust PI-MVT- H∞ controller Based on MVT approach applied to the PMSM drive

Dissertation Submitted in Partial Fulfillment of the Requirements for the Master

&

Publicly defended in: 23/09 /2025

Board of Examiners:

Dr. Ma'amir Madihah	**Chairman**
Dr. Hamidani Bilal	**Supervisor**
Dr. Allag Mariam	**Examiner**

Academic Year: 2024/2025

ملخص

تُستخدم المحركات المتزامنة ذات المغناطيس الدائم (PMSMs) على نطاق واسع في تطبيقات السيارات والتطبيقات الصناعية نظرًا لكفاءتها العالية وصغر حجمها وأدائها الديناميكي الممتاز. ومع ذلك، فإن ديناميكيتها غير الخطية، وعدم اليقين في معاملاتها، وحساسيتها للاضطرابات الخارجية تجعل التحكم فيها صعبًا للغاية.

تتناول هذه الرسالة هذه التحديات من خلال دراسة نهج تحكم هجين يجمع بين تنظيم التناسب والتكامل (PI)، وإطار نظرية القيمة المتوسطة (MVT)، والتحكم المتين H∞. في الفصل الأول، تم وضع النموذج الرياضي لـ PMSM وتحليل أدائه تحت التحكم المتجهي مع العاكس وبدونه. في الفصل الثاني، تم تطبيق طريقة MVT على PMSM، وتحويل النظام غير الخطي إلى نموذج متغير المعاملات الخطية (LPV)، وتؤكد نتائج المحاكاة فعالية هذا النهج. في الفصل الثالث، تم عرض تصميم وحدة التحكم PI-MVT-H∞. تدمج هذه الاستراتيجية الهجينة بساطة التحكم بالتفاعلات الجزيئية (PI)، وقدرات معالجة النظام غير الخطية لـ MVT، ومتانة تحسين H∞.

على الرغم من عدم إجراء أي تحقق تجريبي، إلا أن هذا العمل يوفر أساسًا نظريًا متينًا لتطوير وحدات تحكم PMSM متينة. تمثل المنهجية المقترحة توجهًا واعدًا لتطبيقات مستقبلية مثل محركات المركبات الكهربائية، والروبوتات، والأنظمة الصناعية الدقيقة.

الكلمات المفتاحية: المحركات المتزامنة ذات المغناطيس الدائم ، MVT، التحكم المتين (H∞)، ، التحكم الشعاعي.

Abstract

Permanent Magnet Synchronous Motors (PMSMs) are widely used in automotive and industrial applications due to their high efficiency, compactness, and excellent dynamic performance. However, their nonlinear dynamics, parameter uncertainties, and sensitivity to external disturbances make their control particularly challenging.

This thesis addresses these challenges by investigating a hybrid control approach that combines Proportional–Integral (PI) regulation, the Mean Value Theorem (MVT) framework, and $H\infty$ robust control. In Chapter 1, the mathematical model of the PMSM is established and its performance is analysed under vector control with and without inverter. In Chapter 2, the MVT method is applied to the PMSM, transforming the nonlinear system into a Linear Parameter Varying (LPV) model, and simulation results confirm the effectiveness of this approach. In Chapter 3, the design of the PI–MVT–$H\infty$ controller is presented. This hybrid strategy integrates the simplicity of PI control, the nonlinear system handling capabilities of MVT, and the robustness of $H\infty$ optimization.

Although no experimental validation has been performed, the work provides a solid theoretical basis for the development of robust PMSM controllers. The proposed methodology represents a promising direction for future applications such as electric vehicle drives, robotics, and precision industrial systems.

Keywords: PMSM, MVT, $H\infty$ Control, Robust Control, Vector Control.

Acknowledgement

I first want to prostrate thanking **ALLAH** Almighty for giving me the courage and the patience to complete this work in good conditions.

I would like to express my sincere gratitude to my supervisor **Dr. HAMIDANI BILAL** for his encouragement and guidance throughout the study. I also thank him not only for his technical assists but for his friendship in due course of development of the thesis.

A big thank goes to the Department of Electrical Engineering and the College of Engineering at the University of **Hamma Lakhdar** in El Oued for offering me the opportunity to pursue this Master study.

Dedication

To my dear parents,

To my brothers and sisters

In memory of my grandparents,

To my uncles, aunts, and cousins,

And to all who count for me.

Tables of contents

Public introduction

Chapter 01: Modeling and simulation of permanent magnet synchronous machine

Chapter 02: MVT Control theory

Chapter 03: Robust PI-MVT H∞

Public conclusion & Future works

Appendixes

Lists of figures & tables

a)- List of figures:

b)- List of tables:

Lists of Nomenclatures & Abbreviations

a)- List of Nomenclatures:

B_r:	Remanent flux density
θ:	Angular position (Rotor position)
$\theta(0)$:	Initial Angular position
$V_{a,b,c}$:	Voltage of a,b,c axis
$I_{a,b,c}$:	Current of a,b,c axis
ω:	Rotor angular speed
τ:	Time constant
R_s:	Phase resistance
$\lambda_{a,b,c}$:	Flux linkage of a,b,c phase
$L_{aa,bb,cc}$:	Self-inductance of phase a,b,c
$L_{ab,bc,ac}$:	Mutual-inductance of phase a,b,c
$\lambda_{ma,mb,mc}$:	Phase flux linkage provided by rotor magnet
$I_{d,q}$:	Current of direct (d) and quadrature (q) axis
P_{abc}:	Power of a,b,c phase
P_{dq0}:	Power of direct (d) and quadrature (q) axis
V_{dq0}:	Voltage of direct (d) and quadrature (q) axis
λ_{dq0}:	Flux linkage of direct (d) and quadrature (q) axis
ω_e:	Rotor Electrical angular speed
λ_{pm}:	Permanent magnet flux linkage
L_{dq0}:	Direct (d) and quadrature (q) axis Inductance
P_{in}:	Input power
P_{out}:	Output power
ω_r:	Rotor Mechanical angular speed
P:	Pairs number of pole
T:	Torque

T_e:	Electromagnetic Torque
k:	Numeric constant
i_{ref}:	Reference current
V_{ref}:	Reference voltage
V_{dc}:	Direct voltage
J:	Inertia
$x(t)$:	State vector
$e(t)$:	State estimation vector
$u(t)$:	Input vector
$y(t)$:	Output vector
K_0:	Controller's gain

b)- List of Abbreviations:

PMSM:	Permanent magnet synchronous machine
PI:	Porportional integral
IPM:	Interior permanent magnet
EPM:	Exterior permanent magnet
PM:	Permanent magnet
BLAC:	Brushless Alternative Current
BLDC:	Brushless Direct Current
EMF:	Electro-motive Force
FOC:	Field orientation of control
DC:	Direct current
AC:	Alternative current
SPWM:	Sinusoidal pulse width modulation
PWM:	Pulse width modulation
VSI:	Voltage Source Inverter
SDRE:	State dependent Riccati equation
LPV:	Linear parameter varying
MVT:	Mean value theorem

LMI: Linear matrix inequality

DTC: Direct Torque Control

PDC: Parallel distributed compensator

CFS: Continuous fuzzy systems

General introduction

Permanent Magnet Synchronous Motors (PMSMs) are increasingly used in modern automotive and industrial applications due to their high efficiency, excellent dynamic response, and high power density [1]. Despite these advantages, PMSM control remains challenging because of their nonlinear dynamics, dependence on machine parameters, and susceptibility to external disturbances [2], [3].

Classical Proportional–Integral (PI) controllers are widely applied thanks to their simplicity and steady-state error elimination [4]. However, they suffer from degraded performance when subjected to parameter variations, load disturbances, or un modelled dynamics [5]. Nonlinear control methods such as sliding mode control improve robustness but introduce undesired phenomena such as chattering [2]. On the other hand, robust H∞ control provides strong disturbance rejection and guaranteed stability margins, but its implementation can be computationally demanding [6], [7].

To address these limitations, this thesis investigates a hybrid control approach, the PI–MVT–H∞ controller, which combines three complementary components:

- PI regulation, ensuring structural simplicity and steady-state performance [4].
- Mean Value Theorem (MVT)–based modeling, which transforms PMSM nonlinearities into a Linear Parameter Varying (LPV) framework [8].
- H∞ control, which guarantees robust stability and disturbance rejection in the presence of uncertainties [3], [6].

The contribution of this work lies in the design methodology of the PI–MVT–H∞ controller. Although no experimental validation is included, the thesis develops the theoretical design framework, supported by PMSM modeling and simulation studies. The proposed controller offers a well-balanced solution that overcomes the limitations of conventional PI and nonlinear controllers, making it attractive for applications such as electric vehicle drives, robotics, and high-precision manufacturing [9], [5].

Thesis Structure

This thesis is organized as follows:

- Chapter 01 presents the mathematical modeling of the PMSM, followed by simulation results of vector control strategies with and without inverter.
- Chapter 02 introduces the Mean Value Theorem (MVT) control theory and provides simulation results, demonstrating its effectiveness in handling PMSM nonlinearities.
- Chapter 03 develops the design of the PI–MVT–H∞ controller, combining PI regulation, MVT-based linearization, and H∞ robust control into a unified control framework.
- Finally, the Conclusion and Future Works summarize the main contributions and outline possible research perspectives.

References:

[1] Holtz, J. (2002). "Sensorless Control of Induction Motor Drives." Proceedings of the IEEE, 90(8), 1359-1394.

[2] Khalil, H.K. (2002). Nonlinear Systems (3rd ed.). Prentice Hall.

[3] Chen, B.-S., Lee, T.-S., & Feng, J.-H. (2014). "Robust H∞ Control Design for PMSM Drives with Parameter Uncertainties." IEEE Transactions on Industrial Electronics, 61(5), 2265-2274.

[4] Åström, K.J., & Hägglund, T. (2006). Advanced PID Control. ISA – The Instrumentation, Systems, and Automation Society.

[5] Pillay, P., & Krishnan, R. (1989). "Modeling, Simulation, and Analysis of Permanent-Magnet Motor Drives, Part II: The Permanent-Magnet Synchronous Motor Drive." IEEE Transactions on Industry Applications, 25(2), 274-279.

[6] Zhou, K., & Doyle, J.C. (1998). Essentials of Robust Control. Prentice Hall.

[7] Skogestad, S., & Postlethwaite, I. (2005). Multivariable Feedback Control: Analysis and Design. Wiley.

[8] Liu, H., Li, S., & Wang, H. (2018). "Mean Value Theorem-Based Robust Control for PMSM Drives with Nonlinearities." IEEE Transactions on Power Electronics, 33(6), 5235-5247.

[9] Bose, B.K. (2006). Power Electronics and Motor Drives: Advances and Trends. Academic Press.

Chapter 01

Modeling and simulation of permanent magnet synchronous machine

1.1. Introduction:

Currently, a broad range of industrial and residential drive applications, from high-performance drives to general-purpose drives, use Permanent Magnet Synchronous Machines (PMSM). They are superior to the other kinds of motors in many ways. They are more efficient than induction motors. Additionally, because powerful and reasonably priced magnet materials are now available, PMSMs have high torque-to-volume ratios, high power densities, and high air-gap flux densities.

PMSM is being utilized more and more in high-performance applications that call for highly accurate speed controllers, like industrial machinery and robots [1]. For this reason, a number of control strategies have been developed in recent years. The most often used vector control approach is because it can produce fast dynamic responses and high-performance control characteristics.

Due to the complexity and nonlinearity of PMSMs, a great deal of research has been published describing control and performance issues. The classical proportional integral (PI) controller is still the preferred option in the majority of applications because of its ease of implementation; however, PI controllers are unable to effectively address many real-world issues because of load disturbances, un-modeled states, parameter variations, and friction forces [2].

1.2. Structure of PMSM:

Rotor permanent magnets and stator phase windings are used in the construction of PMSM. The permanent magnets create a steady air gap magnetic field. A three-phase inverter topology is used to externally commutate stator windings. Below Fig. 1.01.

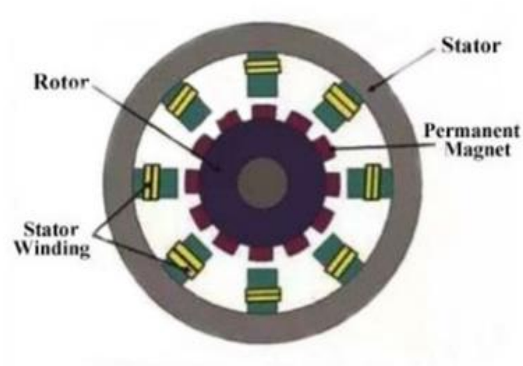

Figure 1.01: The structure of a PMSM.

depicts a PMSM's structure. When the rotor's magnetic vector is perpendicular to the stator's magnetic vector, the torque generated by the interaction of the two magnetic fields reaches its maximum [3]. When building a speed controller, synchronous motors with a prominent rotor can also take advantage of reluctance torque in addition to electromagnetic torque. PMSM falls into a number of categories, which are explained in the part that follows.

1.2.1. Types of PMSM:

Typical PMSMs fall into one of two categories: Interior Permanent Magnet (IPM) motors, where the permanent magnets are concealed inside the rotor (Fig. 1.03), or Exterior Permanent Magnet (EPM) motors, where the permanent magnets are directly facing the air gap and stator armature winding (Fig. 1.02).

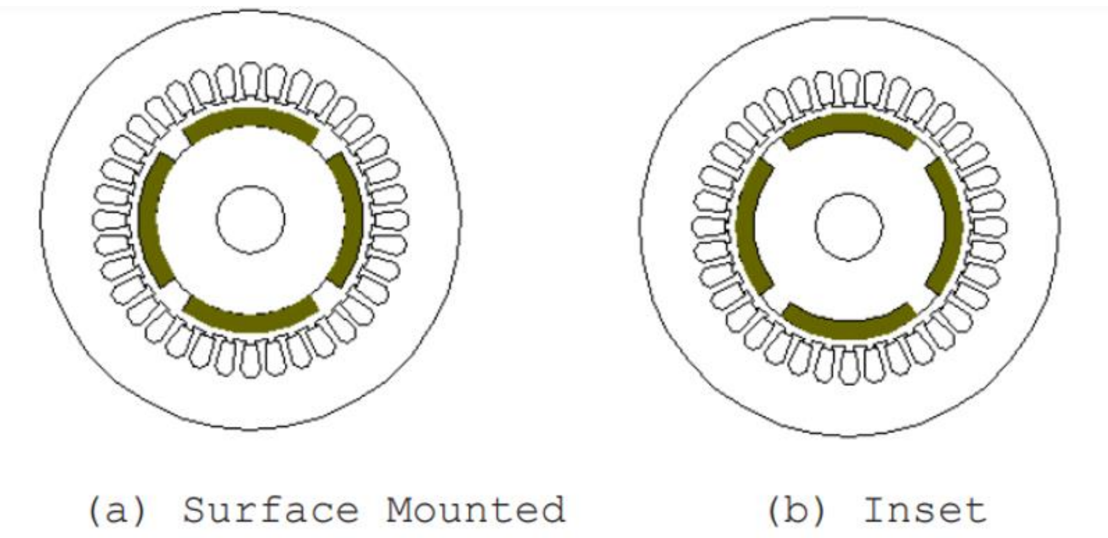

Figure 1.02: Structures of the exterior PMSM.

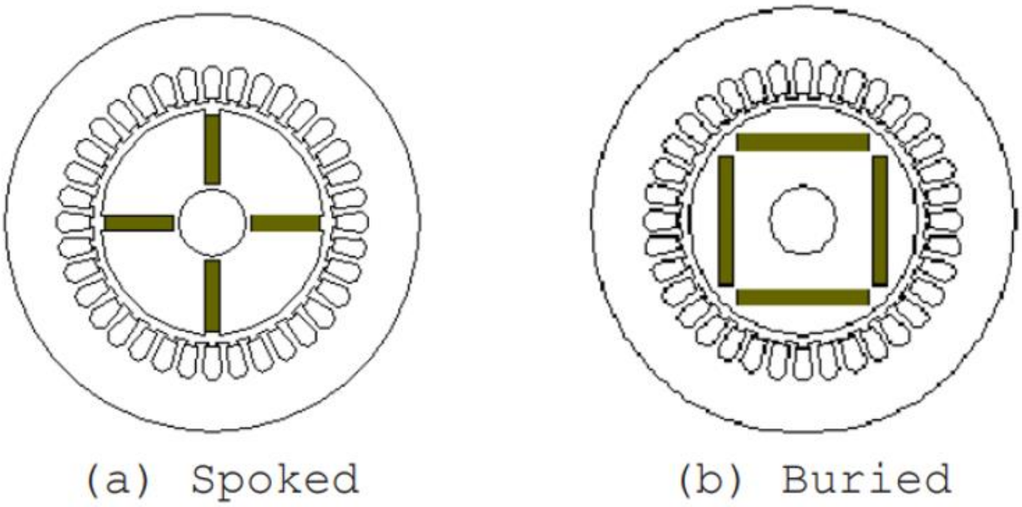

Figure 1.03: Structures of the interior PMSM.

Magnets can be radially magnetized on the surface-mounted PMSM (Fig. 1.2a) in EPM motors. In addition to providing an asynchronous starting torque and serving as a damper, an external high conductivity non-ferromagnetic cylinder can be utilized to shield the magnets from the demagnetizing effects of centrifugal forces and armature response [4]. The permanent magnets in the inset-type motors (Fig. 1.02b) are magnetized.

both radially and within shallow slots. The rotor magnetic circuit may be composed of solid steel or laminate. The d-axis synchronous reactance is smaller than the q-axis synchronous reactance when permanent magnets are present. The permanent magnets' back EMF is less than that of surface-mounted PM rotors due to the rotor's leakage flux. Fig. 1.03a shows that the spoked-magnet rotor of IPM motors has deep slots with circumferentially magnetized magnets. It is imperative that a non-ferromagnetic shaft be applied. IPM motors buried-magnet rotor features magnets that are alternatively poled (Fig. 1.03b). Given that the area of the magnet pole is less than that of the rotor surface, an open circuit, the air gap flux density is lower than the magnet's flux density. Since the armature flux in the q-axis can flow through the steel pole pieces without passing through the PMs, the synchronous reactance in the d-axis is less than that in the q-axis. [5] The magnets are extremely well-protected from centrifugal forces.

Table 1.01 provides a quick comparison of interior and exterior magnet synchronous motors.

Exterior PMSMs	Interior PMSMs
Simple motor construction	Relatively complicated motor construction
Air gap magnetic flux density is smaller than B_r	Air gap magnetic flux density can be greater than B_r
Small armature reaction flux	Higher armature reaction flux
PMs not protected against armature field	PMs protected against armature field
Low PM flux leakage	Higher PM flux leakage
Poor flux-weakening capability	Large flux-weakening capability
Medium speed range	Wide speed range

Table 1.01: Comparison of interior and exterior magnet synchronous motors.

Brushless Alternative Current (BLAC) and Brushless Direct Current (BLDC) are two further classifications for permanent magnet machines based on the type of back-EMF waveform generated in the stator windings. In BLAC machines, a sinusoidal current excitation and a 120° magnet span produce a sinusoidal back-EMF. In contrast, trapezoidal back-EMF is accomplished in BLDC machines through the use of square wave current excitation and a 180° magnet span. Figure 1.04 displays the waveforms of the excitation current and back-EMF for the two types.

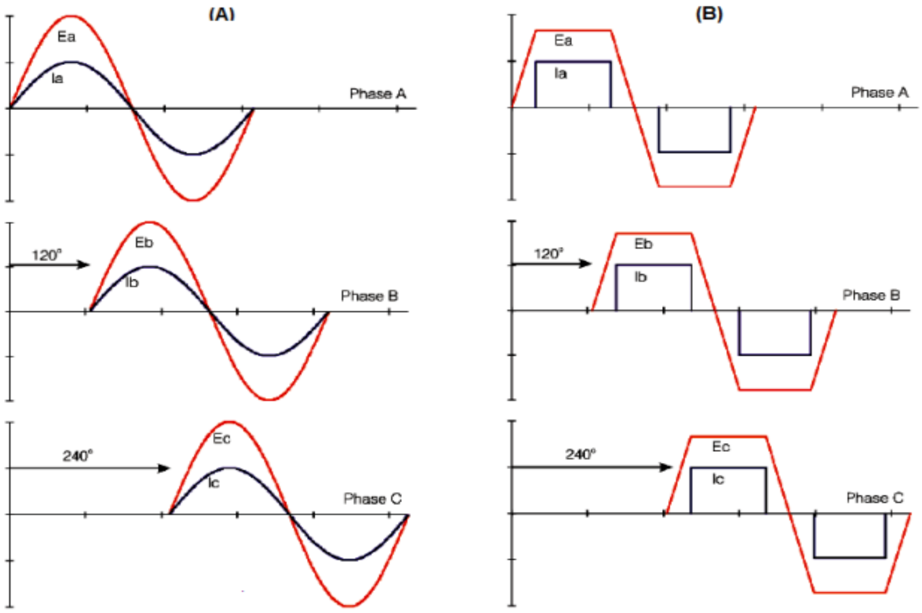

Figure 1.04: Back-EMF voltages and current excitation(A) BLAC, (B) BLDC.

Because the BLDC machine makes better use of the magnetic circuit, it has a higher torque density than the BLAC. The torque and current smoothness of BLDC drives are superior to those of BLAC drives, nevertheless. Its strong torque ripple is caused by switching harmonics and back-EMF. [6]

1.2.2. Design of PMSM:

There has been a lot of work done in the past on the design of PMSMs with different rotor configurations. SLEMON [7,8] established some basic design models for exterior PMSMs for torque capability, loss calculation, thermal properties, and magnet protection. PANIGRAHI [9] provided a detail design example of a surface-mounted PMSM. The design procedure suggested in these papers developed approximate relations for determining the major motor dimensions to meet a design specification. These relations are helpful in obtaining an estimate of what can be achieved before detailed motor design is carried out. However, the majority of the design relations are expressed in a way that is independent of the properties of the inverter supply to the motor.

Although these PM motors may achieve very high torque and acceleration, especially within the usual speed range, their inadequate magnet protection and flux-weakening capability make them unsuitable for high-speed operation. As an alternative to external PMSMs, interior PMSMs with rotor saliency ($L_q / L_d > 1$) might provide attractive performance features and flexibility in adopting different rotor designs, such as spoked or buried magnets [10].

Since the magnets are physically contained and protected inside the rotor, burying them there lays the foundation for a mechanically strong rotor structure that can reach high speeds. When steel pole parts are added, the machine's magnetic circuits are essentially changed, which modifies the torque producing properties of the motor. The rotor saliency can be exploited to lower the PM excitation flux needs in the inner PMSMs in order to achieve extended - speed operating ranges [11, 12].

For the traditional interior PMSM design (Fig. 1.03b), the rotor saliency ratio can reach up to 2 to 3 [13]. Several unusual rotor configurations can be used to attain the necessary motor characteristics [14, 15, 16, 17]. As demonstrated in Fig.1.05 [14], it has been demonstrated that sandwiching flexible magnet sheets between axial laminations can result in a high saliency ratio and a low PM excitation flux. This construction's wide range of steady power speed and low PM flux are advantages.

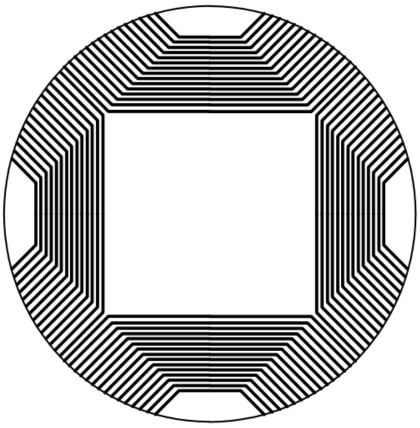

Figure 1.05: Axial laminated rotor cross section for internal PMSM [16].

1.3. Modeling of PMSM:

1.3.1. Reference frame transformation:

Reference frame transformation is a concept used to remove all rotor position-dependent inductances from the voltage equations of the synchronous machine, making the machine model less complex and easier to control. Electric circuits in relative motion and electric circuits with changing magnetic reluctance are the causes of the position-dependent inductances that are present in the synchronous machine model [18].

The transformation uses a frame of reference that rotates at an arbitrary rotational velocity to refer to machine variables. The three-phase a-b-c variables are converted into orthogonal d-q components by transformation.

The introduction of various transformation strategies is contingent upon the reference frame's rotational speed. To support this thesis, a synchronous reference frame that spins in time with the stator variables' basic angular velocity is employed. One can choose the synchronous reference frame's d-q axis orientation in a variety of ways. As demonstrated in our example, the d-axis component is chosen so that it is 90 degrees behind the a-axis, so that at t = 0, the q-axis is aligned with the phase a-axis in fig. 1.06.

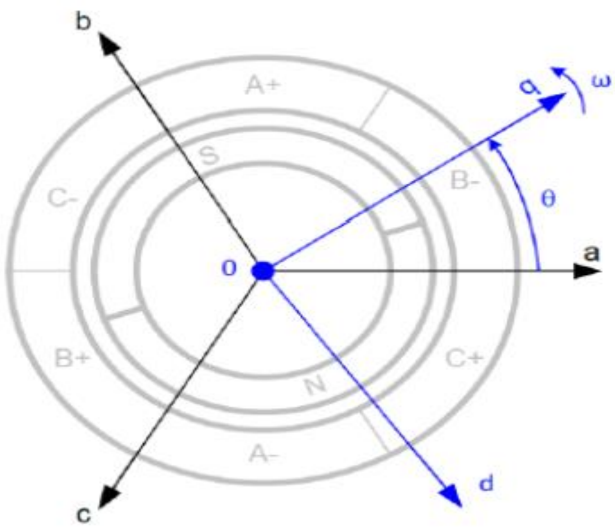

Figure 1.06: Axis orientation d and q axis.

Where The relationship between the synchronous reference frame ω velocity and angular location θ is provided in:

$$\theta(t) = \int_0^t \omega(\tau)d\tau + \theta(0) \tag{1.01}$$

And $\theta(0)$ is the angle between q axis and phase a-axis at t = 0.

$$V_a = R_s I_a + \frac{d\lambda_a}{dt}$$
$$V_b = R_s I_b + \frac{d\lambda_b}{dt} \tag{1.02}$$
$$V_c = R_s I_c + \frac{d\lambda_c}{dt}$$

where phase voltage, current, and resistance are denoted by the symbols (V_a, V_b, V_c), (I_a, I_b, I_c), and R, respectively. The equations for the phase flux linkage (λ_a, λ_b, and λ_c) are [19]:

$$\lambda_a = L_{aa}I_a + L_{ab}I_b + L_{ac}I_c + \lambda_{ma}$$
$$\lambda_b = L_{ba}I_a + L_{bb}I_b + L_{bc}I_c + \lambda_{mb} \tag{1.03}$$
$$\lambda_c = L_{ca}I_a + L_{cb}I_b + L_{cc}I_c + \lambda_{mc}$$

where (λ_{ma}, λ_{mb},λ_{mc}) denotes the permanent magnet-provided phase flux linkage component. The inductances in these equations depend on the angle zero.

Because mutual inductances are at their highest when the rotor q-axis is halfway between two phases, stator self-inductances are at their highest when the rotor q-axis is aligned with the phase axis. In the meantime, the permanent magnet's effect on flux linkage at the stator windings is:

$$\lambda_{ma} = \lambda_m \, cos(\theta)$$

$$\lambda_{mb} = \lambda_m \, cos\left(\theta - \frac{2\pi}{3}\right) \qquad (1.04)$$

$$\lambda_{mc} = \lambda_m \, cos\left(\theta + \frac{2\pi}{3}\right)$$

variables of (a-b-c) may be used to express the power of a three-phase system as:

$$P_{abc} = V_a I_a + V_b I_b + V_c I_c \qquad (1.05)$$

No matter whether reference frame is used to evaluate it, the total instantaneous power remains constant. Since q-d-o variables can be used to express total power as:

$$P_{dq0} = \frac{3}{2}(V_d I_d + V_q I_q + V_0 I_0) \qquad (1.06)$$

The selection of the constant utilized in the transformation is what causes the 3/2 factor. [20]

1.3.2. Modeling of d-q axis:

The synchronous speed of the motor is determined by the speed of the d-q axis reference frame, as previously mentioned, for reference frame transformation. Fig. 1.07 illustrates the selection of the direct axis along the permanent magnetic flux vector. With the use of encoder readings positioned on the rotor shaft, angle θ is determined.

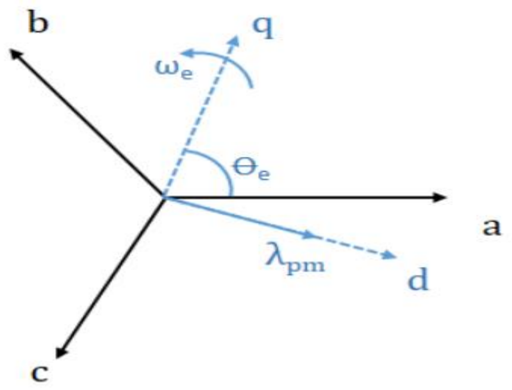

Figure 1.07: D-axis alignment with the PMSM's magnetic flux vector.

1.3.2.1. Voltage and flux equations:

The voltage equation can be written as follows in a synchronous reference frame:

$$V_{dq0} = R_s I_s + \frac{d\lambda_{dq0}}{dt} + \omega_e \lambda_{qd0} \tag{1.07}$$

λ_{dq0} may be acquired as:

$$\lambda_{dq0} = \begin{bmatrix} -\lambda_q \\ \lambda_d \\ 0 \end{bmatrix} \tag{1.08}$$

And the definition of a flux equation is:

$$\lambda_{dq0} = \lambda_{pm,dq0} + L_{dq0} I_{dq0} \tag{1.09}$$

The flux linkage that the permanent magnet causes is denoted by λ_{pm}. The d-q reference frame is selected so that the rotor flux axis and the d-axis line up. Thus, there is no persistent magnet flux along the q-axis.

We can change eq (1.08) to get:

$$\lambda_{dq0} = \begin{bmatrix} -\lambda_q \\ \lambda_d \\ 0 \end{bmatrix} = \begin{bmatrix} -L_q I_q \\ \lambda_{pm} + L_d I_d \\ 0 \end{bmatrix} \tag{1.10}$$

The induction matrix is provided by:

$$L_{dq0} = \begin{bmatrix} L_q & 0 & 0 \\ 0 & L_d & 0 \\ 0 & 0 & L_0 \end{bmatrix} \tag{1.11}$$

After determining that L_d and L_q are the d and q axis stator self-inductances.

The d-axis and q-axis voltage equations can be obtained as follows [3]:

$$\begin{aligned} V_d &= R_s I_d + \frac{dL_d I_d}{dt} - \omega_e (L_q I_q) \\ V_q &= R_s I_q + \frac{dL_q I_q}{dt} - \omega_e (\lambda_{pm} + L_d I_d) \end{aligned} \tag{1.12}$$

Here, ω_e is the electrical angular velocity, $\theta_e$is the electrical angle, and R_s is the stator resistance per phase.

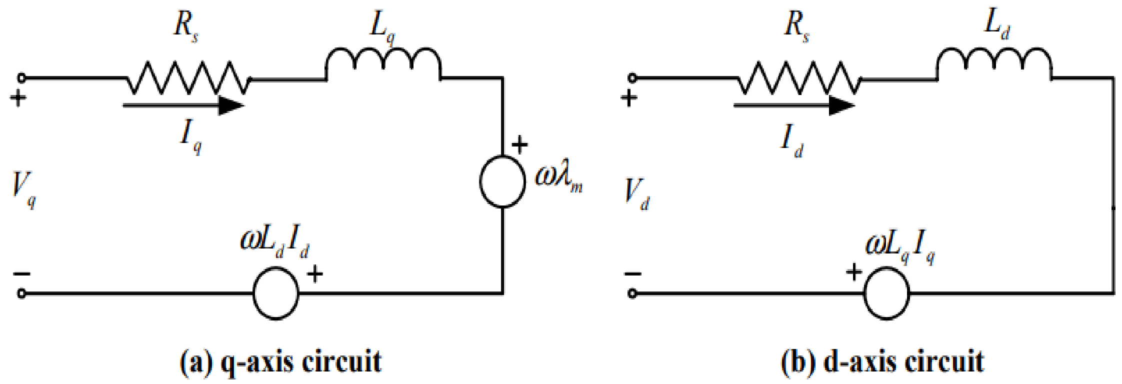

Figure 1.08: Equivalent Circuit of an interior PMSM.

1.3.2.2. Park transformation:

Generally, the performance and behavior of three-phase machines are defined and evaluated using the voltage and current equations. The machines' dynamic behavior is described by time-varying differential equation coefficients, with the exception of the presence of a motionless rotor. The system is challenging to model analytically because of its relative motion, which causes constant variations in the flux links, currents, and induced voltages. When analyzing intricate electrical machinery, mathematical transformations are typically employed to decouple or separate the variables and solve equations involving time-varying values by referring to a common reference frame that may be fixed or rotating.

The Park transformation and the Clarke transformation are the two most popular transformation methods. Selecting the reference frame carefully can significantly reduce the complexity of the machine's mathematical model [21, 22]. As required by the two-axis PMSM model, the voltages V_d and V_q can be converted from the three-phase values (V_a, V_b, V_c) [23].

To convert the three-phase voltages to d-q voltages, Park's transformation is applied. provides a description of Park transformation:

$$\begin{bmatrix} V_d \\ V_q \\ V_0 \end{bmatrix} = \frac{3}{2} \begin{bmatrix} cos(\theta) & cos(\theta - \frac{2\pi}{3}) & cos\left(\theta + \frac{2\pi}{3}\right) \\ -sin(\theta) & -sin(\theta - \frac{2\pi}{3}) & -sin(\theta + \frac{2\pi}{3}) \\ \frac{1}{2} & \frac{1}{2} & \frac{1}{2} \end{bmatrix} \begin{bmatrix} V_a \\ V_b \\ V_c \end{bmatrix} \tag{1.13}$$

And park inverse is [24]:

$$\begin{bmatrix} V_a \\ V_b \\ V_c \end{bmatrix} = \begin{bmatrix} cos(\theta) & -sin(\theta) & 1 \\ cos\left(\theta - \frac{2\pi}{3}\right) & -sin(\theta - \frac{2\pi}{3}) & 1 \\ cos\left(\theta + \frac{2\pi}{3}\right) & -sin(\theta + \frac{2\pi}{3}) & 1 \end{bmatrix} \begin{bmatrix} V_d \\ V_q \\ V_0 \end{bmatrix} \tag{1.14}$$

1.3.2.3. Torque equation:

In a synchronous reference frame, the torque equation can be obtained using the power equation. The d-q axes represent the input power as follows:

$$P_{in} = \frac{3}{2}\left(V_d I_d + V_q I_q\right) \tag{1.15}$$

By changing the voltages and flux connections on the d and q axes in Eq. (1.15),

$$\begin{aligned} P_{in} &= \frac{3}{2}\left[\left(R_s I_d + \frac{d\lambda_d}{dt} + \omega_e \lambda_q\right) I_d + \left(R_s I_q + \frac{d\lambda_q}{dt} \omega_e \lambda_d\right) I_{dq}\right] \\ &= \frac{3}{2}\left[R_s\left(I_d^2 + I_q^2\right) + I_d \frac{d\lambda_d}{dx} + I_q \frac{d\lambda_q}{dx} + \omega_e \lambda_d I_q + \omega_e \lambda_q I_d\right] \end{aligned} \tag{1.16}$$

The fluctuation in magnetic energy is represented by the second two terms, whereas the stator copper losses are represented by the first term. Because of this, the final two terms stand for the mechanical output power that generates the output torque. [20]

$$P_{out} = \frac{3}{2}\omega_e[\lambda_d I_q - \lambda_q I_d] \quad (1.17)$$

Once λ_d and λ_q are entered into Eq. (1.17)

$$P_{out} = \frac{3}{2}\omega_e[\lambda_{pm} I_q - (L_d - L_q)I_d I_q] \quad (1.18)$$

There is a link between output torque and output power.

$$P_{out} = T\Omega \quad (1.19)$$

The motor's electrical and mechanical speeds are connected as follows:

$$\omega_e = P\Omega \quad (1.20)$$

where P represents the quantity of pole pairs.

Equation (1.18) can be changed to yield the torque equation using the relationships mentioned above

$$T = \frac{3}{2}P[\lambda_{pm} I_q - (L_d - L_q)I_d I_q] \quad (1.21)$$

1.4. Field orientation control of PMSM:

Because of the coupling between several factors, the motor control in a PMSM is very nonlinear. To provide decoupling control of stator current, Field oriented control (FOC) divides it into two-phase d-q axis currents: torque producing current (I_q) and field producing current (I_d). This enables independent control of the motor's torque and flux. The PMSM model becomes linear with vector control [25].

$$I_{ds} = 0 \quad (1.22)$$

$$\lambda_d = L_d I_d + \lambda_{pm} \quad (1.23)$$

$$\lambda_q = L_q I_q \quad (1.24)$$

Field orientation serves as the foundational element for PMSM drive control. Since the PM rotor's magnetic flux is fixed with respect to the rotor shaft position, the shaft position sensor can detect the flux position in the coordinates. In (1.24), the d-axis flux linkage λ_d is fixed when I_d= 0. Since λ_{pm} is constant for a PMSM, closed-loop control determines I_q, which in turn determines the electromagnetic torque [28].

$$T_e = \frac{3}{2} P \lambda_{pm} I_q \tag{1.25}$$

Thus, the following is the representation: [29]

$$T_e = k I_q \tag{1.26}$$

And:

$$k = \frac{3}{2} P \lambda_{pm} \tag{1.27}$$

1.5. Inverter:

Direct current (DC) can be converted to alternating current (AC) via an electronic device called an inverter. By converting DC power to AC, sinusoidal pulse width modulation (SPWM) generates the three-phase voltage and current for the motor. $i_{abc,ref}$(t), and V_{dc}(t) from the battery are the inputs of the SPWM, and the three-phase current/voltage i_{abc}(t)/ v_{abc}(t) is the output. Following the generation of a triangle wave carrier signal, s(t), at frequency f_s, a PWM signal is produced by comparing the carrier signal with the reference signal (i_{ref} from the controller).

$$\text{PWM}=\begin{cases} V_{dc}, \text{for } s(t) \geq i_{abc,ref}(t), \\ -V_{dc}, \text{for } s(t) < i_{abc,ref}(t), \end{cases} \tag{1.28}$$

The PWM is in charge of regulating the voltage that is delivered to the motor. In Figure 1.09, equation (1.28) is plotted. The PWM resolution is unaffected because the carrier signal's frequency and the control system's frequency are same. The model excludes the inverter since the PWM frequency is set to a level that makes it possible to assume that the output from the inverter is an ideal three-phase signal [7].

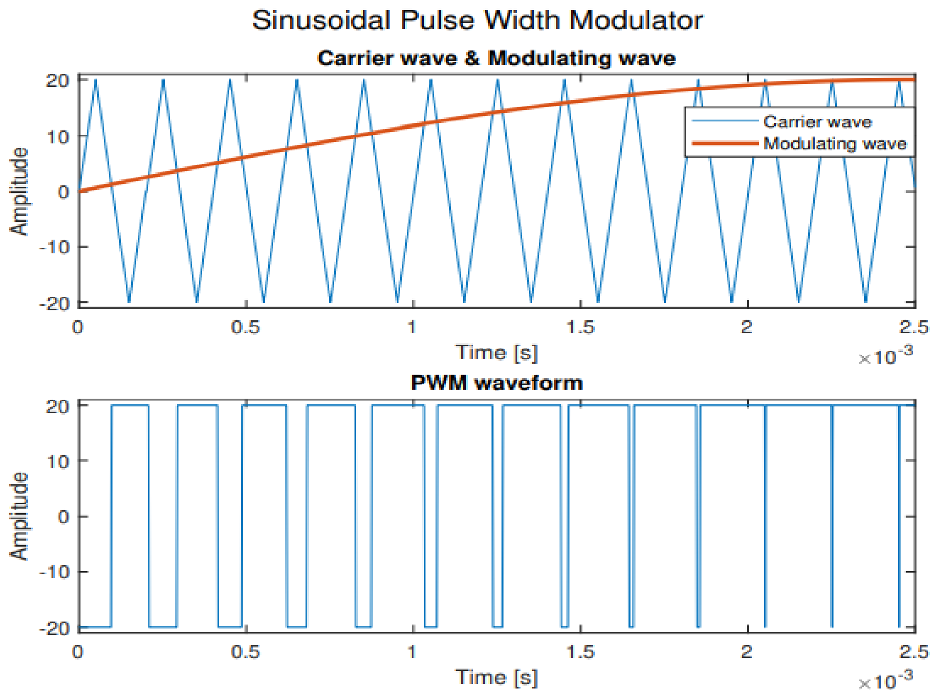

Figure 1.09: An example of the PWM generation process using a reference signal and a carrier.

1.5.1. Pulse width modulation techniques:

In order to control the output voltage of a Voltage Source Inverter (VSI), the most popular method is called pulse width modulation (PWM). The goal of PWM is to create gating pulses for the inverter switches to produce an output voltage with the desired fundamental amplitude and frequency.

1.5.2. Modulation of Sinusoidal Pulse Width:

SPWM is a modulation technique that determines the switching states of the inverter switches by comparing a sinusoidal signal with a high-frequency triangular carrier wave. The upper switch is activated if the reference voltage V_c exceeds the carrier voltage V_c. The lower switch is activated when V_{ref} is less than V_c. The DC-link voltage V_{dc} is the triangle carrier wave's peak-to-peak value. The SPWM technique for producing inverter output voltage is shown in Fig. 1.10.

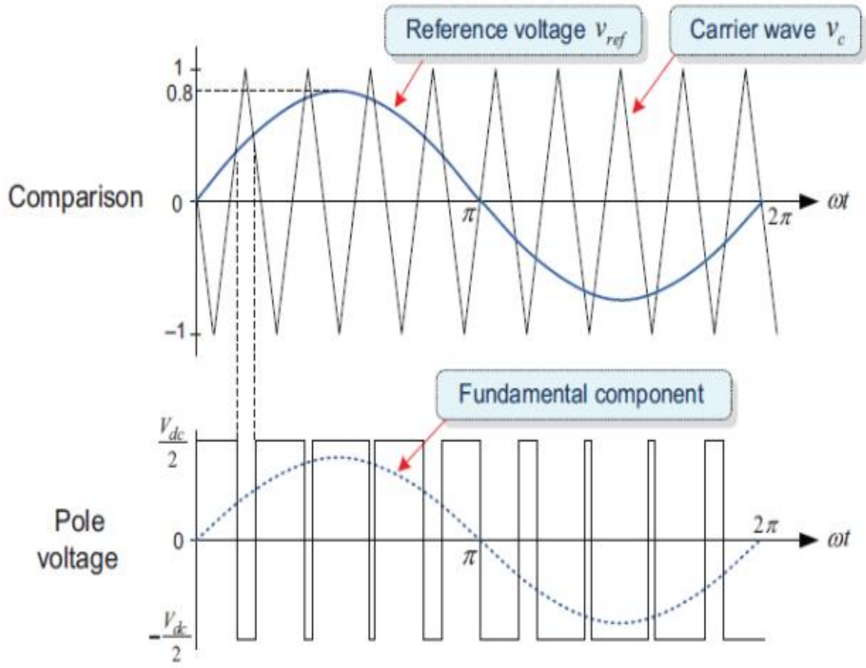

Figure 1.10: Sinusoidal PWM for the Generation of Voltage Waveforms [8].

The modulation index $m = \frac{V_{ef}}{V_{dc}/2}$ must be less than 1 to ensure linear PWM operation. Since the carrier frequency equals the inverter's switching frequency, a constant switching rate is achieved. A higher switching frequency improves waveform quality but increases switching losses, requiring a trade-off between performance and efficiency.

1.6. Simulation results:

1.6.1. Open loop PMSM simulation:

In this part, the simulation of the PMSM under open-loop control is carried out. The motor is first started under no-load conditions, and at t = 1 sec a load torque of 5 N.m is applied to the shaft. The simulation results presented include the rotor speed, the *d*- and *q*-axis stator currents, as well as the three-phase stator currents.

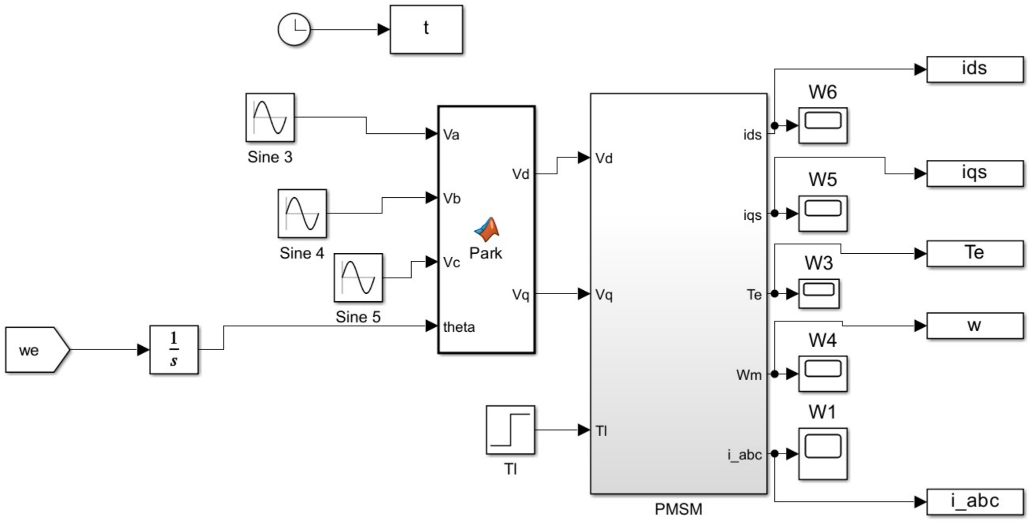

Figure 1.11: Open loop diagram of PMSM.

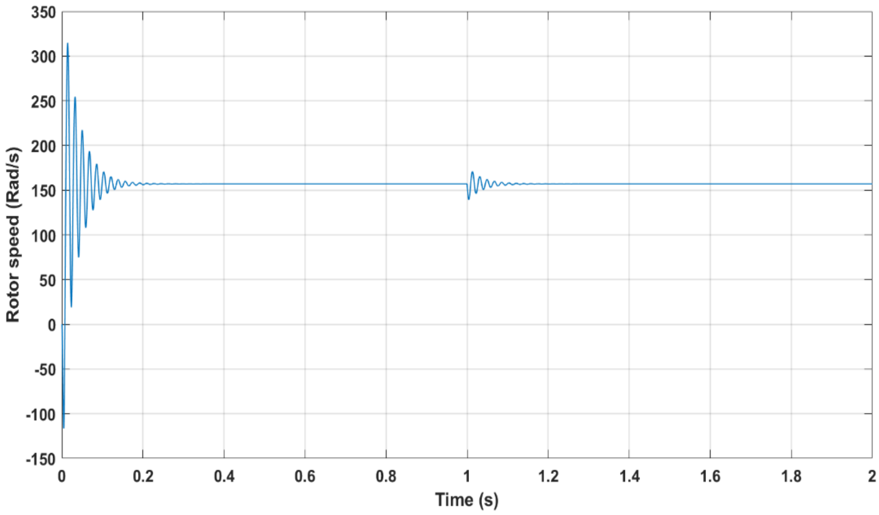

(a)

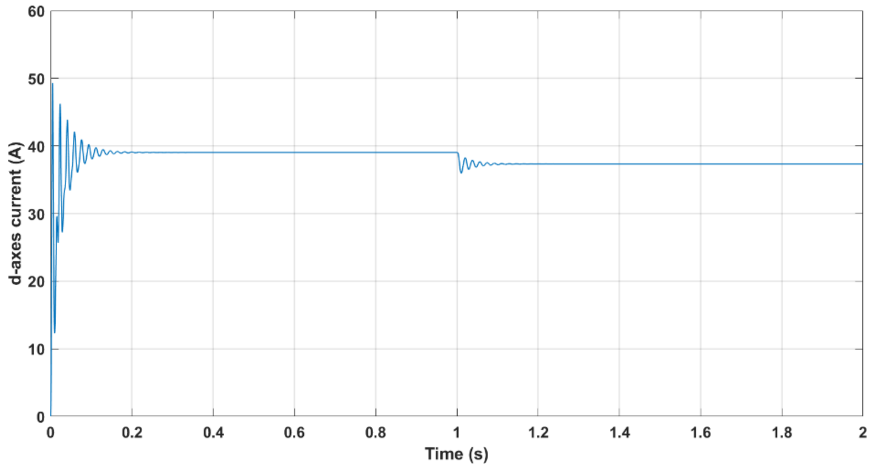

(b)

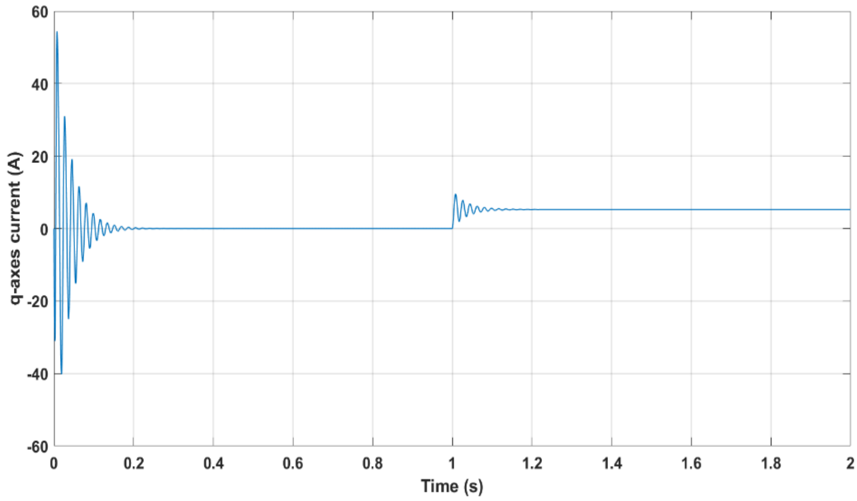

(c)

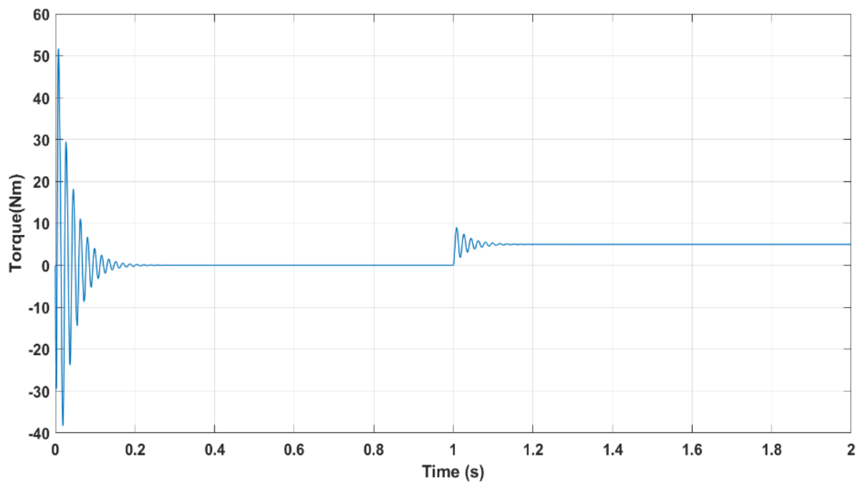

(d)

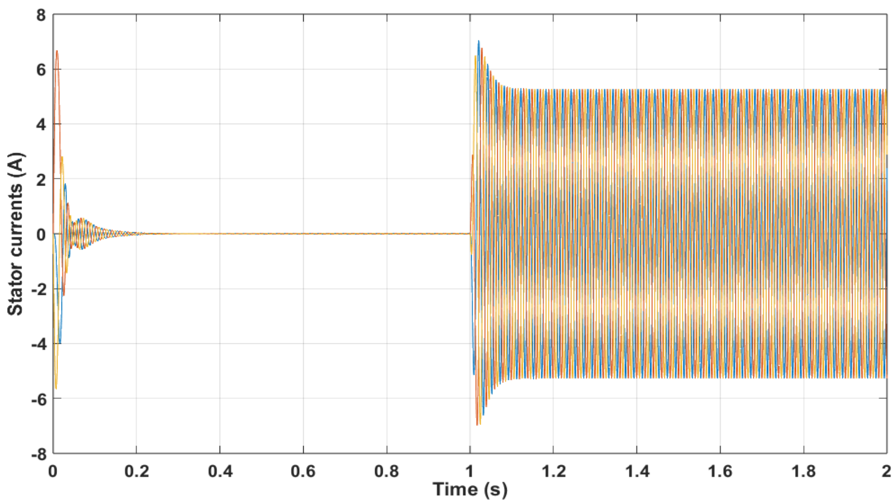

(e)

Figure 1.12: Simulation results of open loop control applied to the PMSM.

1.6.2. FOC of PMSM simulation results:

In this part, the Field-Oriented Control (FOC) of the PMSM is simulated under different operating conditions. The desired rotor speed is initially set to 100 rad/s, then increased to 150 rad/s at t = 1.5 sec. At t = 3 sec, the speed reference is inverted to –100 rad/s. A load torque of 5 Nm is applied at t = 1 sec in order to evaluate the system's response under disturbance. The obtained results present the real and desired rotor speed, the d and q-axis stator currents, as well as the three-phase stator currents, both without and with a PWM inverter.

a) Without PWM Inverter:

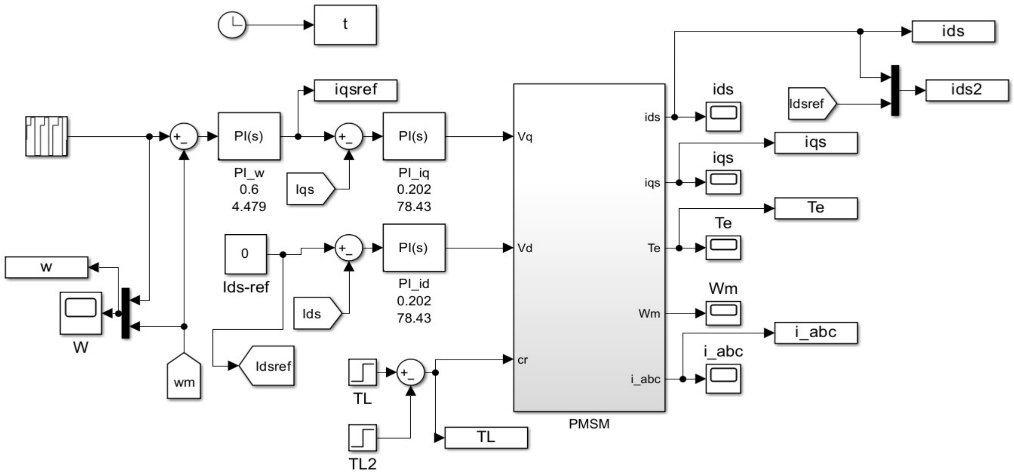

Figure 1.13: FOC design of PMSM without PWM inverter.

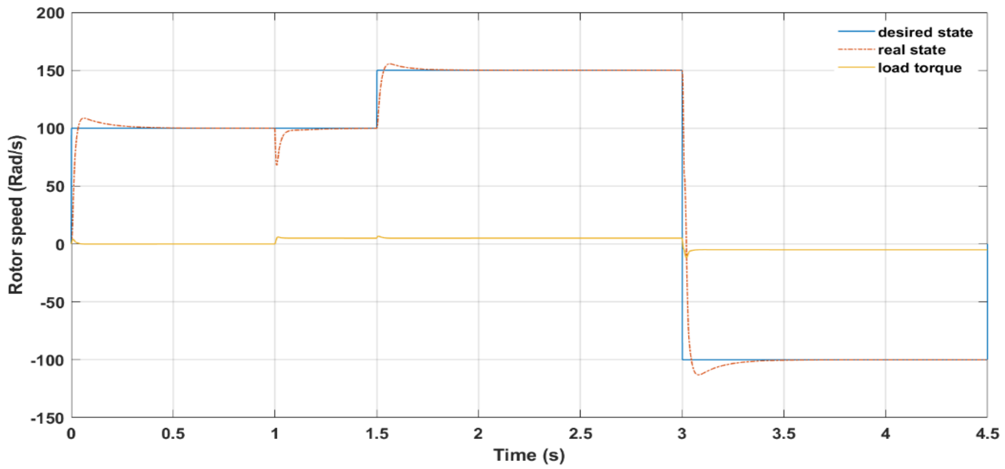

(a) Real and desired rotor speed.

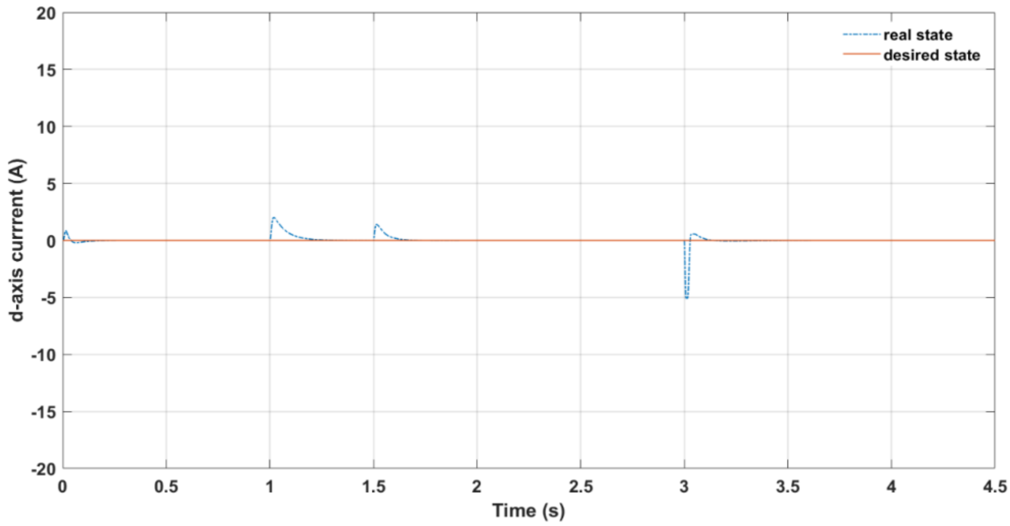

(b) Real and desired d-axis stator current.

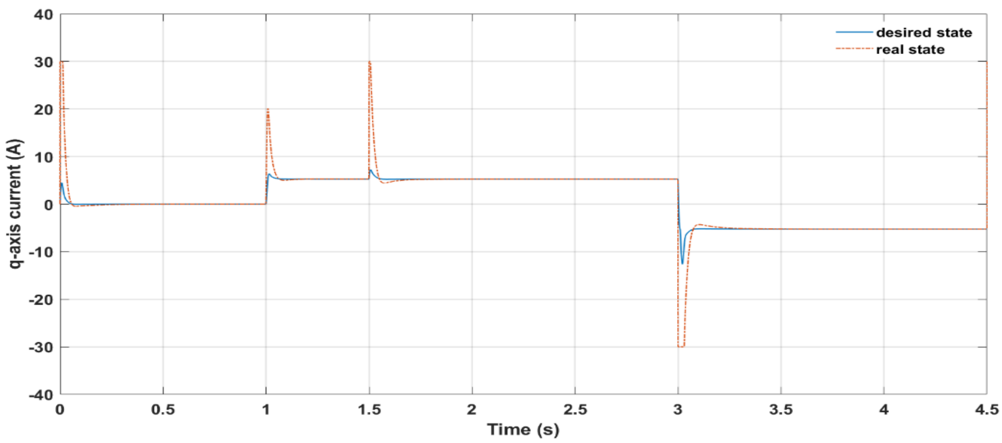

(c) Real and desired q-axis stator current.

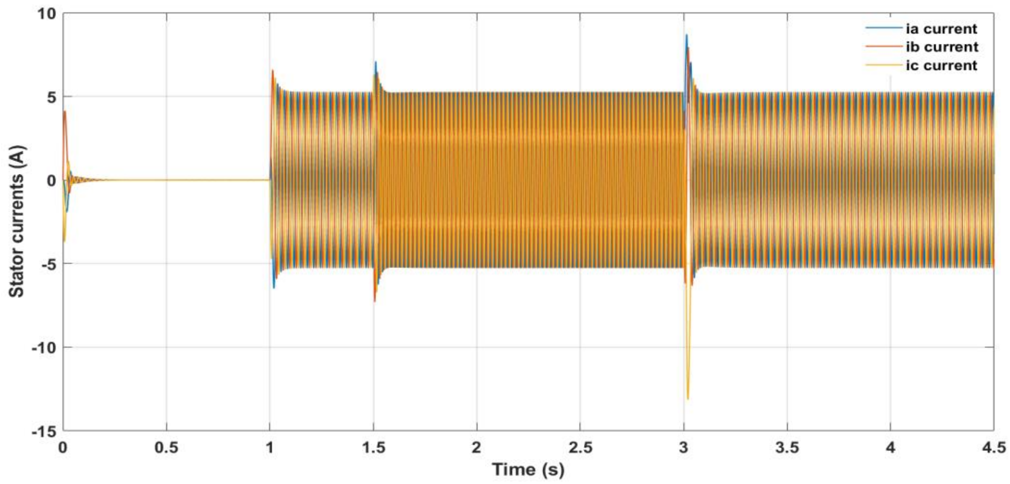

(d) Three phase stator current.

Figure 1.14: Simulation results of FOC control applied to the PMSM without PWM inverter.

b) With PWM Inverter:

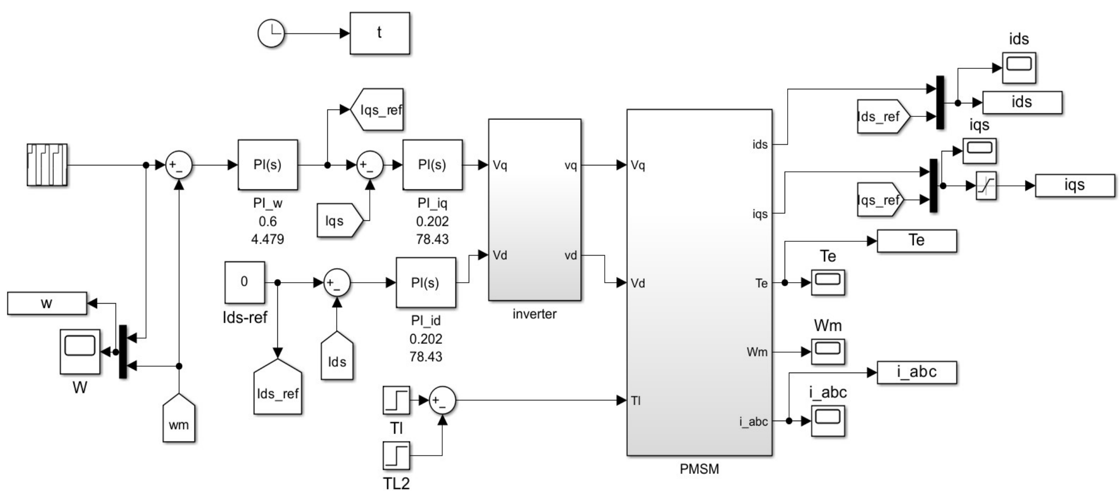

Figure 1.15: FOC design of PMSM with PWM inverter.

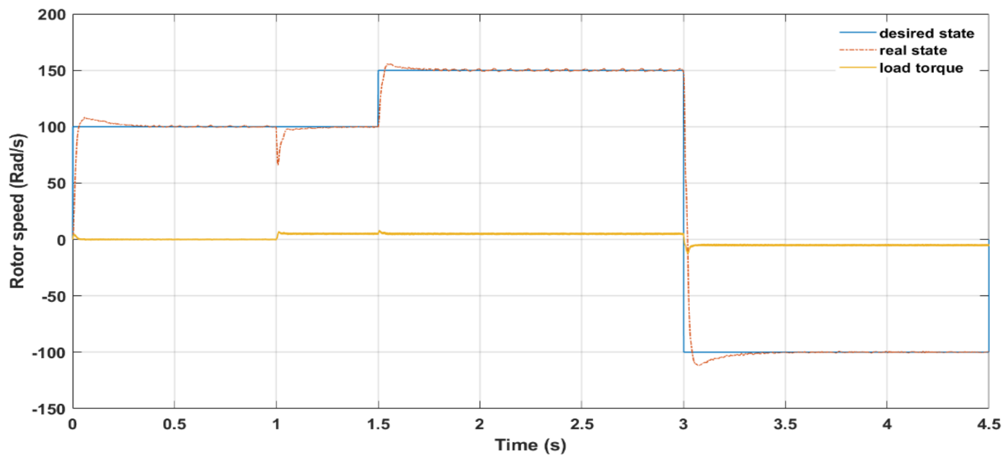

(a) Real and desired rotor speed.

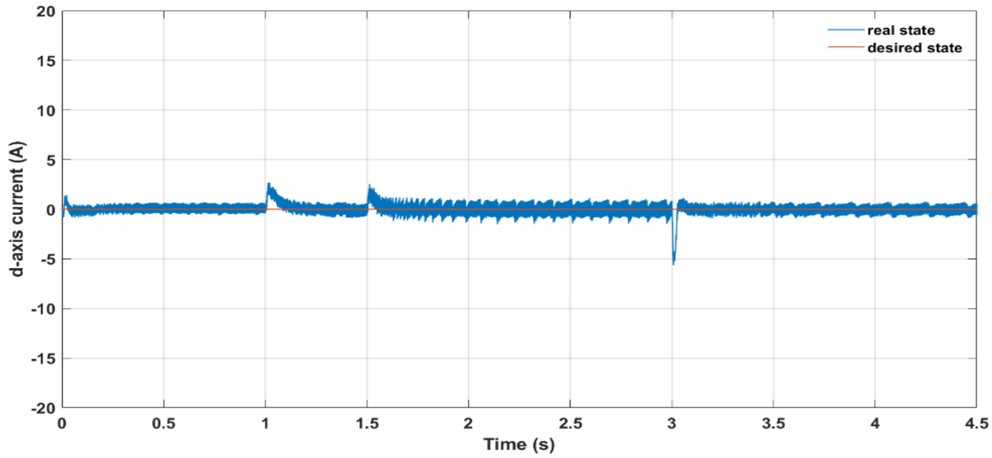

(b) Real and desired d-axis stator current.

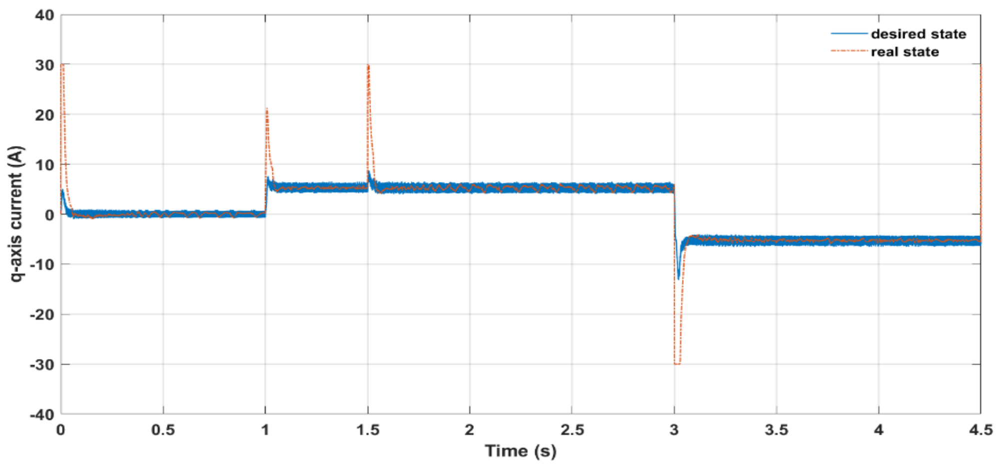

(c) Real and desired q-axis stator current.

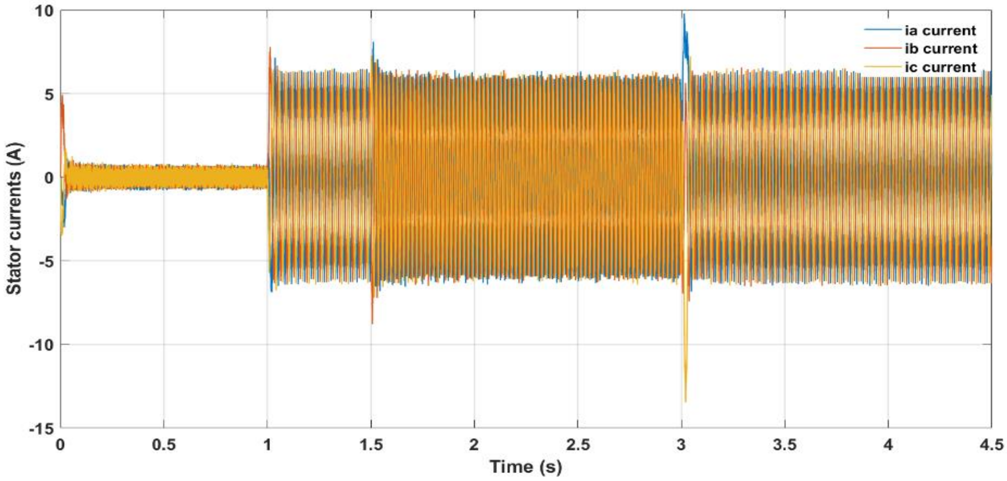

(d) Three phase stator current.

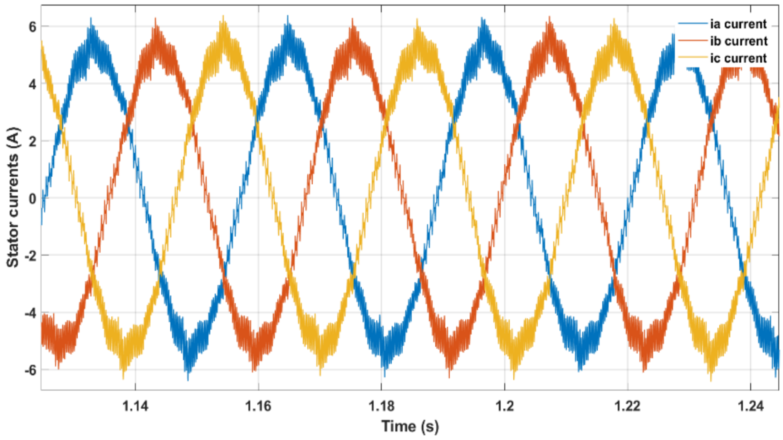

(e) Zoom

Figure 1.16: Simulation results of FOC control applied to the PMSM with PWM inverter.

1.6.3. Global discussion of PMSM simulation results:

The simulation results show the difference in performance between open-loop control and Field-Oriented Control (FOC) of the PMSM. In figure 1.12 which represents the open-loop case, the rotor speed and stator currents are not well regulated, leading to oscillations and poor dynamic response. This confirms the limitation of open-loop strategies, especially under varying load conditions. With FOC, the decoupling of flux and torque is achieved, and both d- and q-axis currents closely follow their references. Without the PWM inverter (figure 1.14), the current waveforms appear ideal and sinusoidal, which highlights the effectiveness of the control algorithm in theory. However, when the PWM inverter is introduced (figure 1.16), the currents exhibit switching harmonics and ripple due to the modulation process, although the average values remain aligned with their references. The rotor speed tracks the desired reference accurately in both FOC cases, demonstrating good dynamic and steady-state performance. The zoomed view in the PWM case further illustrates the presence of high-frequency components, but the control remains robust. Overall, the results confirm that FOC provides excellent control of PMSM torque and speed, with the PWM inverter introducing realistic distortions while maintaining satisfactory performance.

1.7. Conclusion:

In conclusion, this chapter has presented the mathematical modeling of the Permanent Magnet Synchronous Motor (PMSM) and its associated control strategies. The fundamental equations of the machine were established, forming the basis for simulation and analysis. Different control approaches were then applied in order to evaluate the behavior of the PMSM under various operating conditions. The obtained simulation results confirmed the validity of the developed models and illustrated the effectiveness of advanced control methods. This work provides a clear understanding of PMSM dynamics and lays the groundwork for the design of efficient drive systems.

1.8. References:

[1] Harshada V. Deo, International Journal of Innovative Research in Technology, Vol.11(1), 2014 A Review of Speed Control Techniques Using PMSM.

[2] X. Zhang, Li. Sun, K. Zhao, and L. Sun. Nonlinear Speed Control for PMSM System Using Sliding-Mode Control and Disturbance Compensation Techniques In IEEE Transactions on Power Electronics, volume 28, pages 1358–1365, Mar 2013.

[3] Field Oriented Control of Permanent Magnet Synchronous Motors User's Guide, Microsemi

[4] M. Satoh, M. Tomita, and S. Kanedo, "Comparison between SPM motors and IPM motors for compressors of air-conditioners," IPEC, Tokyo, pp. 1286–1289, 2000.

[5] T. M. Jahns, "Interior permanent-magnet synchronous motors for adjustable- speed drives," IEEE Transactions on Industry Application, vol. IA-22, pp. 738–746, July/August 1986.

[6] Adam Walker, Lecture slides: Permanent Magnet Motor Drives, University of Nottingham

[7] G. R. Slemon, "On the design of high-performance surface-mounted pm mo- tors," IEEE Transaction on Industry Application, vol. 30, pp. 134–140, Jan- uary 1994.

[8] G. R. Slemon and X. Liu, "Modelling and design optimization of permanent magnet motors," Electric Machines and Power Systems, vol. 20, pp. 71–92, 1992.

[9] B. P. Panigrahi and K. C. Patra, "Design of a permanent magnet synchronous motor," Electric Machine and Power System, vol. 27, pp. 771–779, 1999.

[10] L. Qinghua, M. A. Jabbar, and A. M. Khambadkone, "Design optimisation of wide-speed permanent magnet synchronous motors," in Proceedings of International Conference on Power Electronics, Machines and Drives, (Bath, UK), pp. 404–408, April 2002

[11] L. Qinghua, M. A. Jabbar, and A. M. Khambadkone, "Design optimisation of interior permanent magnet synchronous motors for wide-speed operation," in Proceedings of The 4th IEEE International Conference on Power Electronics and Drive Systems, (Bali, Indonesia), pp. 475–478, October 2001.

[12] L. Xu and L. Ye, "A new design concept of permanent magnet machine for flux weakening operation," IEEE Transaction on Industry Application, vol. 31, pp. 373–378, March/April 1995.

[13] R. Krishnan, Electric Motor Drives: Modeling, Analysis, and Control. Prentice Hall, 2001.

[14] W. L. Soong, D. A. Staton, and T. J. E. Miller, “Design of a new axially- laminated interior permanent magnet motor,” IEEE Transaction on Industry Application, vol. 31, pp. 358–367, Mar/Apr 1995.

[15] D. M. Ionel, J. F. Eastham, and T. Betzer, “Finite element analysis of a novel brushless dc motor with flux barriers,” IEEE Transacion of Magnetics, vol. 31, pp. 3749–3751, November 1995.

[16] N. Bianchi, S. Bolognani, and B. J. Chalmers, “Salient-rotor pm synchronous motors for an extended flux-weakening operation range,” IEEE Transaction on Industry Application, vol. 36, pp. 1118–1125, July/August 2000.

[17] J. C. Teixeira, C. Chillet, and J. P. Yonnet, “ Structure comparison of buried permanent magnet synchronous motors for flux weakening operation, ” Inter-national Conference on Electrical Machines and Drives, pp. 365–370, 1993.

[18] Paul Krause,Oleg Wasynczuk, Analysis of Electric Machinery and Drive Systems, chapter 3. IEEE, 2013

[19] L. W. Matsch and J. D. Morgan, Electromagnetic and Electromechanical Ma- chines. John Wiley and Sons, third ed., 1986.

[20] Sang-Hoon Kim, Electric Motor Control DC, AC and BLDC Motors, chapter 4.2. Elsevier, 2016

[21] J. Pradeep and R. Devanathan, "Adoption of Park's Transformation for Inverter Fed Drive," International Journal of Power Electronics and Drive Systems, 5, 3, 366, 2015.

[22] H. I. Hussein, " Mathematical driving model ofthree phase induction motors in stationary coordinate frame, " Diyala Journal of engineering sciences, 8, 4, 2015.

[23] A. Apte, R. Walambe, V. Joshi, K. Rathod, andJ. Kolhe, "Simulation of a permanent magnetsynchronous motor using Matlab-Simulink," in2014 annual IEEE India conference (INDICON),2014: IEEE, 1.

[24] Y. M. Prajapati and N. K. Jaiswal, " Sensor - lesscontrol of permanent magnet Synchronous motor," in 2019 3rd International Conference on Trends in Electronics and Informatics (ICOEI), 2019: IEEE. 201

[25] Kaushik Jash, Int. Journal of Engineering Research and Applications, Vol.3(5), 2013, Vector Control of Permanent Magnet Synchronous Motor Based On Sinu- soidal Pulse Width Modulated Inverter with Proportional Integral Controller.

Chapter 02

MVT control theory

2.1. Introduction:

High performance servo applications frequently use permanent magnet synchronous motors (PMSM) [1] because of their high power density, high efficiency, and large torque to inertia ratio [2–4]. However, because PMSMs are extremely nonlinear multivariable dynamic systems, it is challenging to precisely manage their speed using traditional control algorithms when load and parameter perturbations occur and speed sensors are not available [5, 6].

Nonlinear speed control methods based on linearization and/or high-frequency switching, such TS fuzzy controls, sliding mode control, feedback linearization control, backstepping, and state dependent Riccati equation (SDRE), have been used to PMSM drives [7].

In order to express the nonlinear error dynamics of the coupled system and controller as a convex combination of known matrices with time variable coefficients as LPV systems, the suggested design technique relies on the mean value theorem (MVT). MVT and sector nonlinearity to nonlinear elements in the equation of state error controller have been used to solve these kinds of issues [8, 9]. Stability requirements are determined and stated in terms of linear matrix inequalities by employing the Lyapunov theory [10, 6] to build the controller gains based on the results for that class of nonlinear systems. Lastly, LMIs are solved to obtain the controller gains [11].

2.2. Mean value theorem:

2.2.1. Mean value theorem for bounded jacobian systems:

A mathematical tool is introduced in this subsection, which will be utilized later to construct the controller gains in the following section. First, the vector function MVT is introduced [12, 8]. Next, the rules for expressing a vector function in composition form are established. The MVT is presented in a modified form for vector functions.

First, the nonlinear vector function's n distinct entries are presented.

$$\emptyset(w): R^{n+p} \rightarrow R^{n} \tag{2.01}$$

They are represented by $\emptyset_i(w)$, which comes after:

$$\emptyset(w): [\, \emptyset_i(w) \ldots\ldots \emptyset_n(w)]^T \tag{2.02}$$

And $\emptyset_i(w)\colon R^{n+p} \to R$ where $i = 1 \ldots\ldots n$ and $w = (x, u) = (w_1, w_2 \ldots\ldots w_{n+p})$

Let's represent $e_n(i)$ as the vector of R^n, where all elements are null except for the i_{th}, which is equal to one.

$$e_n(i) = \begin{bmatrix} 0 \ldots\ldots 0 & 1 & 0 \ldots\ldots 0 \\ 1 \ldots\ldots i-1 & i & i+1 \ldots\ldots n \end{bmatrix} \tag{2.03}$$

We can represent $\emptyset(w)$ as:

$$\emptyset(w) = \sum_{i=1}^{n} e_n(i)\emptyset_i(w) \tag{2.04}$$

Theorem 01:

[8]. Take $\emptyset_i(w)$: $R^{n+p} \to R^n$ as an example. Let a and $b \in R^{n+p}$. For [a, b], if $\emptyset_i(w)$ is differentiable, then $c \in R^{n+p}$ and δ(c) $\in R^{n+p}$ are two constant vectors. fulfilling ξ(c) $\in [x^m, x^m]$ (i.e., ξ(c) $\in [\underline{\xi_{ij}}, \overline{\xi_{ij}}]$) with $\xi^M = (\ldots, \overline{\xi_{ij}}, \ldots)$ and $\xi^m = (\ldots, \underline{\xi_{ij}}, \ldots)$,

for $i = 1 \ldots\ldots n$ and $j = 1 \ldots\ldots n+p$ such that

$$\emptyset_i(a) - \emptyset_i(b) = \frac{\partial \emptyset}{\partial w}(c)(a-b) = \xi_{ij}(c)(a-b)$$
$$= \left(\sum_{i=1}^{n} \sum_{J=1}^{n+p} e_n(i) e_n^T(j) \frac{\partial \emptyset_i}{\partial w_j}(c) \right)(a-b) \tag{2.05}$$

It is possible to obtain Eq. (2.06).

$$\emptyset_i(x(t), u) - \emptyset_i(x_c(t), (u_c(t))) = \frac{\partial \emptyset}{\partial w}(c)(w - w_c)$$
$$= \frac{\partial \emptyset}{\partial w}(c) \begin{bmatrix} x - x_c \\ u - u_c \end{bmatrix} \tag{2.06}$$

And $c \in \left[\left(x_c(t), u_c(t)\right), \left(x(t), u(t)\right)\right]$

Function g(x) will be swapped out for B_0 for PMSM-machine control, and at the nominal equilibrium point (regulation $x_c(t) = 0$),

$$\emptyset\big(x_c(t),(u_c(t)\big) = \Big(f\big(x_c(t)\big) - A_0 x_c(t)\Big) + (g(x) - B_0)u(t) = 0 \qquad (2.07)$$

Eq. (2.06) therefore reduces to

$$\emptyset_i(x(t), u(t)) = \frac{\partial \emptyset}{\partial w}(c)x(t)$$

Furthermore, in the tracking case when $x_c(t)$= stepwise signal and function $\emptyset(x_c(t),(u_c(t)) \neq 0$, Eq. (2.06) can be simplified as

$$\emptyset_i(x(t), u) = \frac{\partial \emptyset}{\partial w}(c)\big(x(t) - x_c(t)\big) + \emptyset_i\big(x_c(t), u_c(t)\big)$$

The MVT indicates that the gradient

$$\left\{\frac{\partial \emptyset}{\partial x}(c) = \sum_{i=1}^{n}\sum_{J=1}^{n} e_n(i)e_n^T(j)\frac{\partial \emptyset_i}{\partial w}(c) \right. \qquad (2.08)$$

The state error equation is obtained by substituting Eq. (2.08).

$$\dot{e} = \left[A_0 - B_0K_0 + \sum_{i=1}^{n}\sum_{J=1}^{n} e_n(i)e_n^T(j)\frac{\partial \emptyset_i}{\partial w}(c)\right]e + \left[B_0K_0x_c + \emptyset_i\big(x_c(t), u_c(t)\big)\right] \qquad (2.09)$$

Premises:

$$\underline{\xi_{ij}} \leq \frac{\partial \emptyset_i}{\partial x_j}(c) = \xi_{ij} \leq \overline{\xi_{ij}} \ ; \overline{\xi_{ij}} \geq \max\left(\frac{\partial \emptyset_i}{\partial x_j}(c)\right) \qquad (2.10)$$

And:

$$\underline{\xi_{ij}} \leq \min\left(\frac{\partial \emptyset_i}{\partial x_j}(c)\right)$$

so that the sector nonlinearity can be used to replace each nonlinearity $\frac{\partial \emptyset_i}{\partial x_j}$ by:

$$\left\{\frac{\partial \emptyset_i}{\partial x_j}(c) = \overline{\delta_{ij}}\,\overline{\xi_{ij}} + \underline{\delta_{ij}}\,\underline{\xi_{ij}} \right. \qquad (2.11)$$

$$\left\{\sum_{i=1}^{n}\sum_{J=1}^{n} e_n(i)e_n^T(j)\frac{\partial \emptyset_i}{\partial x_j}(c) = \sum_{i}^{n}\sum_{J}^{n}(\overline{\delta_{ij}}\,H_{ij}\,\overline{\xi_{ij}} + \underline{\delta_{ij}}\,H_{ij}\,\underline{\xi_{ij}}) \right. \qquad (2.12)$$

so that the functions of weighting system

$$\begin{cases} \delta_{ij}^{1} & = \dfrac{\dfrac{\partial \emptyset_i}{\partial x_j} - \underline{\xi_{ij}}}{\overline{\xi_{ij}} - \underline{\xi_{ij}}} \\ \delta_{ij}^{2} & = \dfrac{\underline{\xi_{ij}} - \dfrac{\partial \emptyset_i}{\partial x_j}}{\overline{\xi_{ij}} - \underline{\xi_{ij}}} \end{cases} \tag{2.13}$$

Where $\sum_{e=1}^{2} \xi_{ij}^{e} = 1$ as $0 \leq \xi_{ij}^{e} \leq 1$

Otherwise, $H_{ij}$is a zeros matrix, unless it takes one in the location indicated with the *i*th raw and *j*th columns. It is possible to obtain Eq. (2.14) by substituting Eq. (2.12) in Eq. (2.09).

$$\dot{e} = \sum_{i=1}^{q} h(\xi)(A_0 - B_0K_0 + A_i)e + \left[B_0K_0x_c + \emptyset_i\big(x_c(t), u_c(t)\big)\right] \tag{2.14}$$

Thus, Eq. (2.14)'s ultimate state can be written as:

$$\dot{e} = \sum_{i=1}^{q} h(\xi)G_i e + \left[B_0K_0x_c + \emptyset_i\big(x_c(t), u_c(t)\big)\right] \tag{2.15}$$

In T-S fuzzy [13, 14] systems, the sector nonlinearity technique defines the weighting functions $h_i(.)$ using the previously defined local weighting functions $\xi_{ij}(.)$. Next, determining the controller gain K_0 that will make the system Eq. (2.15) asymptotically stable is the control design challenge. Thus, the relaxation and results technics in Refs. [14, 9] can be used.

2.2.2. MVT controller design:

The control vector, as per the state feedback control law, is provided by:

$$u(t) = -K_0 e(t) \tag{2.16}$$

where $e_c(t)$is the state error vector, and K_0 is the controller's gain matrix.

$$e_c(t) = x(t) - x_c(t) \tag{2.17}$$

In (2.17), $x_c(t)$ represents the intended states.

The error dynamic equation can be written as follows using (2.17):

$$\dot{e}_c(t) = \dot{x}(t) - \dot{x}_c(t) \tag{2.18}$$

We may write $\dot{x}(t) = 0$ from (2.18) since $x_c\,(t)$ is a stepwise signal:

$$\dot{e}_c(t) = (A_0 - B_0K_0 + A_i)e(t) + \left[\emptyset\big(x(t)\big) - \ \emptyset_i\big(x_c(t)\big)\right] \tag{2.19}$$

The goal is to identify the gain matrix K_0 at which the non-linear Lipchitz system (2.19) reaches asymptotic stability.

The nonlinear component of the Lipchitz system is then subjected to the MVT and the sector nonlinearity transformation. As a result, the system becomes:

$$\dot{e}_c(t) = \left[A_0 - B_0K_0 + \sum_{i=1}^{n}\sum_{J=1}^{n} e_n(i)e_n^T(j)\frac{\partial\emptyset_i}{\partial w}(c)\right]e(t) \tag{2.20}$$

When sector nonlinearity transformation is used, the system (2.20) turns into

$$\dot{e}_c(t) = \sum_{r=1}^{j} \xi_{ij}^r(A_0 - B_0K_0 + A_i)e(t) \tag{2.21}$$

2.2.3. Stability studies:

Eq. (2.15) is examined for stability using the quadratic Lyapunov function of the first term. However, the equation's stability is unaffected by the second component, which operates in the feed forward. With a common matrix to Eq. (2.22) the stability is examined using the quadratic Lyapunov function [11, 15].

$$\dot{e} = \sum_{i=1}^{q}(A_0 - B_0K_0 + A_i)e + \left[B_0K_0x_c + \emptyset_i\big(x_c(t), u_c(t)\big)\right] \tag{2.22}$$

And

$$v\big(e(t)\big) = e^T(t)Pe(t), P = PT > 0$$

The derivative with regard to t so is connected to the stability.

$$\dot{v}\big(e(t)\big) = \ e^T(t)((A_0^TP + PA_0 - K_0^TB_0^TP - PB_0K_0) + A_h^TP + PA_h)e(t) \tag{2.23}$$

And

$$A_h = \sum_{i=1}^{q} h_i(\delta)\, A_i$$

With $q \leq 2^{n^2}$

If Lyapunov Eq. (2.23)'s time derivative is negative definite, the state equation is guaranteed to be stable, resulting in the time-dependent LMIs listed below:

$$(A_0^T P + PA_0 - K_0^T B_0^T P - PB_0 K_0) + A_h^T P + PA_h < 0 \tag{2.24}$$

Time independent inequalities can be obtained thanks to the weighting functions' convex sum property.

$$(A_0^T P + PA_0 - K_0^T B_0^T P - PB_0 K_0) + A_i^T P + PA_i < 0 \tag{2.25}$$

For $i = 1 \ldots, \ldots n$

The change of variables K_0P = M is utilized to describe inequality (2.25) in terms of LMI, and the following conditions of LMI are obtained, where α is the rate of convergence. The dynamics may also exhibit an oscillatory behavior, it should be noted. In an LMI zone, pole assignment can enhance the controller's performance.

Theorem 02:

If P = PT >0, then the closed-loop dynamics (2.22) is asymptotically stable, meaning that

$$(A_0^T P + PA_0 - K_0^T B_0^T P - PB_0 K_0) + A_i^T P + \alpha P < 0 \tag{2.26}$$

for $j = 1, \ldots, r$ and $i = 1, \ldots, q$.

Additionally, in the event that every requirement is met, the controller gain is

$$K_0 = MP$$

2.2.4. Augmented state feedback regulator:

In the presence of disturbances or model uncertainties, the MVT-PI-controller is intended to guarantee zero steady-state tracking error for stepwise reference signals [2, 16]. It works by injecting an essential action into the forward channel, which is a well-known process. Following the introduction of a new state variable to incorporate the tracking error, the expanded modified PDC system controller may be defined as

$$u(t) = [K_0 \quad K_{\mathrm{I}}]\begin{bmatrix} e(t) \\ e(t)_{\mathrm{I}} \end{bmatrix} = \bar{K}\overline{e(t)} \tag{2.27}$$

And $\dot{e}_{\mathrm{I}}(t) = x(t) - x_c(t)$

With state tracking inaccuracy, the augmented system's closed-loop becomes

$$\overline{\dot{e}(t)} = \sum_{i=1}^{q} h_i\,(\mu)(\bar{G}_\iota\overline{e(t)} + \bar{D}_\iota\overline{v(t)}) \tag{2.28}$$

With $\bar{G}_\iota = \bar{A}_\iota - \overline{B_\iota \bar{K}}$

Such that

$$\bar{A}_\iota = \begin{bmatrix} A_0\, A_1 & 0 \\ I & 0 \end{bmatrix} : \bar{B} = \begin{bmatrix} B_0 \\ 0 \end{bmatrix}$$
$$\bar{D}_\iota = \begin{bmatrix} A_0 + A_i & 0 \\ I & 0 \end{bmatrix} : \bar{v}(t) = \begin{bmatrix} x_c(t) \\ C_r(t) \end{bmatrix} \tag{2.29}$$

With load $C_r(t)$

Using selecting a quadratic function that can be solved using an LMI tool in a manner similar to example I, the stability theorem for the augmented system (2.28) and the controller's convergence can be obtained using Lyapunov direct with only minor adjustments to the augmented system's matrices.

Theorem 03:

If P = P^T exists, the augmented system's closed-loop dynamics (2.28) is asymptotically stable, such that

$$(\bar{A}_I^T P + P\bar{A}_\iota - M^T\bar{B}^T - \bar{B}M) + \alpha P < 0 \tag{2.30}$$

for $i = 1, \dots, q$

Furthermore, $\bar{K} = MP^{-1}$ is the controller gain if all the requirements are met.

2.2.5. Mathematic formation of PMSM with closed loop FOC:

2.2.5.1. Dynamic model of PMSM:

The mechanical and electrical systems make up the two components of an AC motor's governing equation.

2.2.5.1.1. Electrical governing equation:

Permanent magnets and stator windings affixed to the rotor surface (surface mounted PMSM) make up the mathematical model of the PMSM. Each phase's voltage, current, and inductance of the PMSM are transmitted to the two d-q axes using the synchronous reference system thesis. The PM synchronous motor's electrical equations can be expressed in the rotor flux reference frame (d-q axis) as [1, 4], which is the rotor rotating reference frame.

$$\begin{aligned} \frac{dI_d}{dt} &= \frac{1}{L_d}u_d - \frac{R}{L_d}I_d - \frac{L_q}{L_d}p\Omega I_q \\ \frac{dI_q}{dt} &= \frac{1}{L_q}u_q - \frac{R}{L_q}I_q + \frac{L_q}{L_d}p\Omega I_d - \frac{\lambda_{pm}}{L_d}p\Omega \\ \frac{d\Omega}{dt} &= \frac{1}{J}(T_e - f\Omega - I_q) \end{aligned} \tag{2.31}$$

2.2.5.1.2. Mechanical governing equation:

The energy conversion process produces torque, which is employed to propel mechanical loads. Its expression is connected to mechanical parameters by the fundamental dynamics law as

$$T_e = 1.5P\left(\lambda I_q + (L_d - L_q)I_d I_q\right) \tag{2.32}$$

The state space of the three-phase PMSM can be defined in the d-q reference frame.

$$\begin{aligned} \dot{x_1} &= \frac{1}{L_d}u_1 - \frac{R}{L_d}x_1 - \frac{L_q}{L_d}px_2x_3 \\ \dot{x_2} &= \frac{1}{L_q}u_2 - \frac{R}{L_q}x_2 + \frac{L_q}{L_d}px_1x_3 - \frac{\lambda_{pm}}{L_d}P\Omega \\ \dot{x_3} &= \frac{3}{2}p\frac{\lambda}{J}x_2 - \frac{f}{J}x_3 - \frac{C_r}{J} \end{aligned} \tag{2.33}$$

And

$$x = [\,x_1 \;\; x_2 \;\; x_3\,]^T = \left[I_d \;\; I_q \;\; \Omega\right]^T ; \; u = [\,u_1 \;\; u_2\,]^T = \left[u_d \;\; u_q\,\right]^T$$

2.2.6. Closed loop field orientation control (CL-FOC):

As seen in Fig.2.01, field orientation control (FOC) is the fundamental idea of PMSM control [16, 17]. This is accomplished by allowing the permanent magnet to

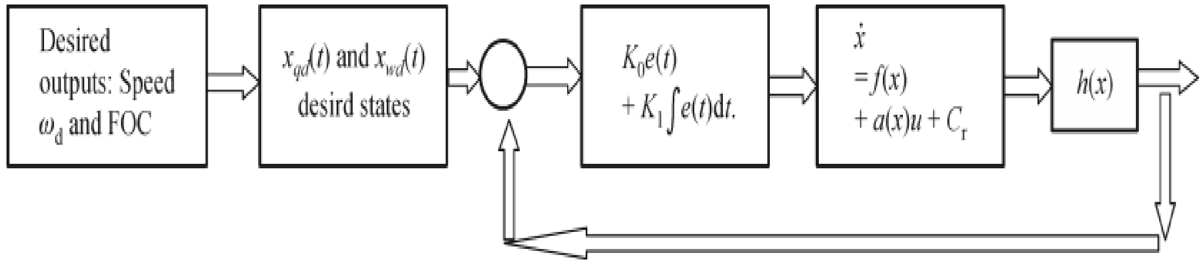

Figure 2.01: MVT-PI-controller principle diagram for closed-loop-FOC PMSM.

The stator torque component vector and flux linkage should line up in the d-axis, while I_q is maintained in the q-axis direction. This indicates that the field orientation is achieved by maintaining the courant id value at zero. Assuring FOC control requires identifying the desired states in order to use the FOC idea in a closed loop.

Assuming a given load torque C_r and a fixed target speed, ω_d, the field orientation condition must be met, meaning that the current aligned in the d-axis must remain zero (x_{dd}=0). Eq. (2.33) would then be used to determine the desired value for the current x_{dq} aligned in the q-axis.

$$\begin{cases} x_{dq}(t) \approx \mathcal{L}^{-1}\left\{\dfrac{\left(J_s + \frac{3}{2}P\frac{\lambda}{J}\right)\Omega_d(s) - \frac{C_r(s)}{J}}{1+\mathrm{t}_2 s}\right\} \\ x_{dq}(t) \approx \mathcal{L}^{-1}\left\{\dfrac{\Omega_d(s)}{1+\mathrm{t}_2 s}\right\} \end{cases} \tag{2.34}$$

2.3. T-S fuzzy:

Fuzzy control systems have been increasingly prominent in engineering applications in recent years. A rush of activity in the analysis and design of systems of fuzzy control has been spurred by the many successful applications of fuzzy control. In order to help control researchers and engineers tackle engineering challenges, we present some of the evaluation and development instruments used in the systems in this chapter.

The Takagi-Sugeno fuzzy model framework and the so-called parallel scattered compensation, a controller structure developed in line with the fuzzy model, serve as the foundation for the toolkit that is provided in this chapter. The fundamental ideas, analysis, and design processes of this methodology are presented in this chapter [16].

In this chapter, the Takagi-Sugeno fuzzy modeling (T-S fuzzy model) is introduced, and then the steps for creating such models are covered. Next is a description of a model-based fuzzy controller architecture that makes use of the idea of "parallel distributed compensation." In order to compensate for each rule in a fuzzy system, the controller design's primary goal is to generate each control rule. The process of design is intuitive and conceptually straightforward. Moreover, this chapter demonstrates how the stability analysis and control design issues can be simplified to LMI issues involving linear matrix inequality.

2.3.1. T-S fuzzy modeling:

A nonlinear system's local linear input-output relationships are represented by fuzzy IF-THEN rules, which characterize the fuzzy model put out by Takagi and Sugeno [17]. Expressing the regional dynamics of each fuzzy consequence (rule) using a linear system model is the primary characteristic of a Takagi-Sugeno fuzzy model. The linear system models are fuzzy "blended" to create the overall fuzzy model of the system. This chapter demonstrates how Takagi-Sugeno fuzzy models can be used to represent a wide variety of nonlinear dynamic systems. Indeed, Takagi-Sugeno fuzzy models have been shown to be universal approximators.

CFS:

If $z_1(t)$ is M_{i1} and … and $z_p(t)$ is M_{ip}.

Then $$\begin{cases}\dot{x}(t) = A_i x(t) + B_i u(t) \\ y(t) = C_i x(t)\end{cases} \quad \text{And } i = 1,2,\dots,r. \tag{2.35}$$

Here, M_{ip} is the fuzzy set and r is the number of model rules; $x(t) \in R^n$ is the state vector, $A_i \in R^{n\times \mathrm{n}}$, $B_i \in R^{n\times \mathrm{m}}$, and $C_i \in R^{q\times n}$; $z_1(t)$,…, $z_p(t)$ are identified premise variables that may be functions of the state variables, $u(t) \in R^{\mathrm{m}}$ is the input vector, $y(t) \in R^q$ is the output vector, external disturbances, and / or time. The vector comprising each of the individual elements $z_1(t)$,…, $z_p(t)$ will be represented by $z(t)$. In this book, it is assumed that the basis variables do not depend on the variables of input $u(t)$. In order to prevent a complex defuzzification procedure for fuzzy controllers, this assumption is required [16].

It should be noted that stability conditions proposed in this book can be used even when the input variables (t) are functions of the premise variables. A "subsystem" is any linear subsequent equation denoted by $A_i x(t) + B_i u(t)$.

The fuzzy systems' final outputs are deduced as follows given a pair of $(x(t), u(t))$:

$$\dot{x}(t) = \frac{\sum_{i=1}^{r} w_i\big(z(t)\big)\{A_i x(t) + B_i u(t)\}}{\sum_{i=1}^{r} w_i\big(z(t)\big)}$$

$$= \sum_{i=1}^{r} h_i\big(z(t)\big)\{A_i x(t) + B_i u(t)\} \tag{2.36}$$

$$y(t) = \frac{\sum_{i=1}^{r} w_i\big(z(t)\big)\{A_i x(t) + B_i u(t)\}}{\sum_{i=1}^{r} w_i\big(z(t)\big)}$$

$$= \sum_{i=1}^{r} h_i\big(z(t)\big) C_i x(t) \tag{2.37}$$

And

$$[z_1(t), z_2(t), \dots \dots, z_P(t)]$$

$$w_i\big(z(t)\big) = \prod_{j=1}^{p} M_{ij}\left(z_j(t)\right)$$

$$h_i\big(z(t)\big) = \frac{w_i\big(z(t)\big)}{\sum_{i=1}^{r} w_i\big(z(t)\big)} \tag{2.38}$$

For every t . The membership level of $z_j(t)$ in M_{ij} is denoted by the word M_{ij} $(z_j(t))$. Given that

$$\begin{cases} \dot{x}(t) = \sum_{i=1}^{r} w_i\big(z(t)\big) > 0 \\ w_i\big(z(t)\big) > 0 \qquad\qquad i = 1,2,\dots,r. \end{cases} \tag{2.39}$$

And

$$\begin{cases} \dot{x}(t) = \sum_{i=1}^{r} w_i\big(z(t)\big) = 1 \\ h_i\big(z(t)\big) \geq 0 \qquad\qquad i = 1,2,\dots,r. \end{cases} \tag{2.40}$$

2.3.2. Fuzzy model construction:

The model-based fuzzy control design technique covered in this chapter is shown in Figure 2.02. We require a Takagi-Sugeno fuzzy example of a nonlinear system in order to construct a fuzzy controller. Thus, creating a fuzzy model is a crucial and fundamental step in this process. The problem of how to create this a fuzzy model is covered in this section. Generally speaking, there are two methods for building fuzzy models:

a) Identification fuzzy modeling with input-output data.
b) Derivation from provided nonlinear system equations.

Fuzzy modeling with input-output data has been extensively studied in the literature since Takagi, Sugeno, and Kang's outstanding work [18, 19]. parameter and Structure identification are the two primary components of the process. Fuzzy modeling using the identification strategy is appropriate.

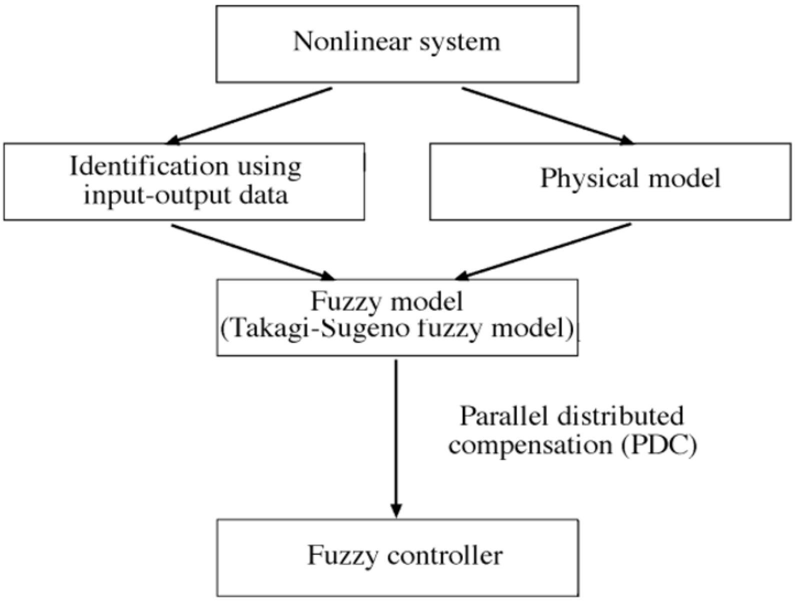

Figure 2.02: Fuzzy control architecture based on a model [17].

For plants whose representation using physical and/or analytical models is impossible or too challenging. Conversely, nonlinear dynamic models for mechanical systems might be easily generated using techniques like the Newton-Euler and Lagrange methods. It is more acceptable in these situations to use the second method, which creates a fuzzy model from supplied nonlinear dynamical models.

In this part, we concentrate on this second strategy. To create fuzzy models, this method makes use of the concepts of "sector nonlinearity," "local approximation," or a mix of the two.

2.3.2.1. Sector nonlinearity:

It was first proposed in [20] to use sector nonlinearity in the building of fuzzy models. The following concept serves as the foundation for sector nonlinearity. Examine the following straightforward nonlinear system: $\dot{x}(t) = f(x(t))$, where $f(0) = 0$. Finding the global sector such that $\dot{x}(t) = f(x(t)) \in [a_1 \ \ a_2]x(t)$ is the goal. Figure 2.03 shows the approach to sector nonlinearity. This method ensures a precise fuzzy model construction. However, for generic nonlinear systems, it can occasionally be challenging to identify global sectors. We can take into account local sector nonlinearity in this situation. This makes sense because physical system variables are always bound. The local sector nonlinearity is displayed in Figure 2.04.

The local sectors under $-d < (t) < d$ are represented by two lines. In the "local" region, the fuzzy model accurately depicts the nonlinear system, which is $-d < (t) < d$. The specific procedures for creating fuzzy models are demonstrated in the example that follows.

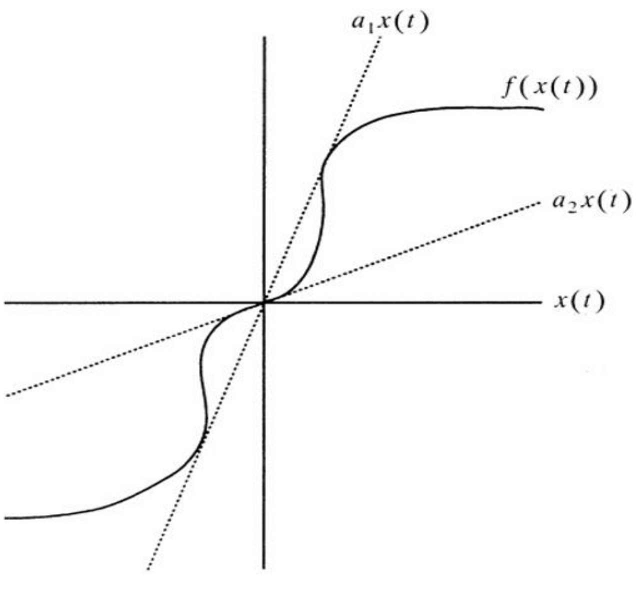

Figure 2.03: Nonlinearity in global sectors [17].

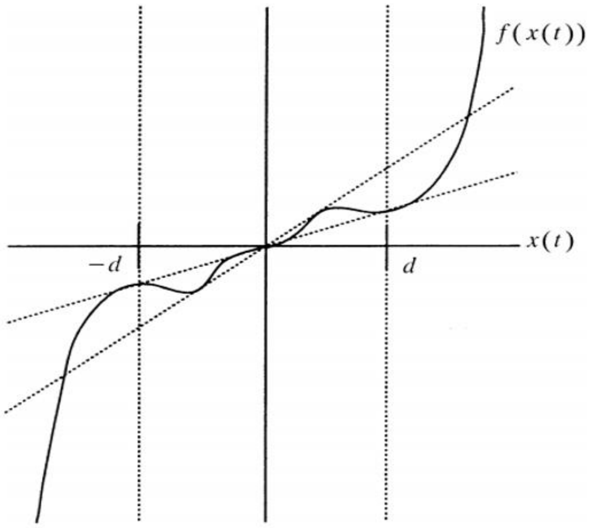

Figure 2.04: Nonlinearity in the local sectors.

Example: nonlinear system below:

$$\begin{pmatrix} \dot{x}_1(t) \\ \dot{x}_2(t) \end{pmatrix} = \begin{pmatrix} -x_1(t) + x_1(t)x_2^3(t) \\ -x_2(t) + \big(3 + x_2(t)\big)x_1^3(t) \end{pmatrix} \tag{2.41}$$

Simply put, we suppose that $x_1(t)$ and $x_2(t)$ are in the $[-1 \quad 1]$ range. Naturally, we can build a fuzzy model by assuming any range for $x_1(t)$ and $x_2(t)$.

One way to express equation (2.07) is as

$$\dot{x}_1(t) = \begin{bmatrix} -1 & x_1(t)x_2^2(t) \\ \big(3 + x_2(t)\big)x_1^2(t) & -1 \end{bmatrix} x(t) \tag{2.42}$$

In which $x(t)$ = $[x_1(t) \;\; x_2(t)\,]^T$ The expressions T and $x_1(t)x_2^2(t)$ and$\big(3 + x_2(t)\big)x_1^2(t)$ are nonlinear. To define the nonlinear terms,

we have $z_1(t)$ = $x_1(t)x_2^2(t)$ and $z_2(t)$ =$\big(3 + x_2(t)\big)x_1^2(t)$.

After that, we have

$$\dot{x}_1(t) = \begin{bmatrix} -1 & z_1(\mathrm{t}) \\ z_2(\mathrm{t}) & -1 \end{bmatrix} x(t) \tag{2.43}$$

Next, under $x_1(t) \in [-1 \ \ 1]$ and x_2(t)$\in [-1 \ \ 1]$, determine the lowest and greatest values of z_1(t)and z_2(t). Here's how to get them:

Max	**Min**
$x_1(t), x_1(t)^{z_1(\mathrm{t})=1}$	$x_1(t), x_1(t)^{z_1(\mathrm{t})=-1}$
Max	**Min**
$x_1(t), x_1(t)^{z_2(\mathrm{t})=4}$	$x_1(t), x_1(t)^{z_2(\mathrm{t})=0}$

Using the highest and lowest values, z_1(t) and z_2(t) can be expressed as

$$z_1(\mathrm{t}) = \ x_1(t)x_2(t)^2 = M_1(z_1(t)) \times (1) + M_2(z_1(t)) \times (-1)$$

$$z_2(\mathrm{t}) = (3 + x_2(t))x_1(t)^2 = N_1(z_1(t)) \times (4) + M_2(z_1(t)) \times (0)$$

And

$$M_1\big(z_1(t)\big) + M_2\big(z_1(t)\big) = 1$$

$$N_1\big(z_2(t)\big) + N_2\big(z_2(t)\big) = 1$$

Consequently, it is possible to compute the membership functions as

$$M_1\big(z_1(t)\big) = \frac{z_1(t)+1}{2} \qquad M_2\big(z_1(t)\big) = \frac{1-z_1(t)}{2}$$

$$N_1\big(z_1(t)\big) = \frac{z_2(t)}{4} \qquad N_2\big(z_2(t)\big) = \frac{4-z_2(t)}{2}$$

The membership functions have been given the names "Positive," "Negative," "Big," and "Small," accordingly. The fuzzy model that follows then represents the nonlinear system (2.41).

Model Rule 1:

IF $z_1(t)$ is Positive and $z_2(t)$ is big.

THEN $\dot{x}(t) = A_1 x(t)$

Model Rule 2:

IF $z_1(t)$ is Positive and $z_2(t)$ is small.

THEN $\dot{x}(t) = A_2 x(t)$

Model Rule 3:

IF $z_1(t)$ is Negative and $z_2(t)$ is big.

THEN $\dot{x}(t) = A_3 x(t)$

Model Rule 4:

IF $z_1(t)$ is Negative and $z_2(t)$ is small.

THEN $\dot{x}(t) = A_4 x(t)$

And

$$A_1 = \begin{bmatrix} -1 & 1 \\ 4 & -1 \end{bmatrix} \qquad A_2 = \begin{bmatrix} -1 & 1 \\ 0 & -1 \end{bmatrix}$$

$$A_3 = \begin{bmatrix} -1 & -1 \\ 4 & -1 \end{bmatrix} \qquad A_4 = \begin{bmatrix} -1 & -1 \\ 0 & -1 \end{bmatrix}$$

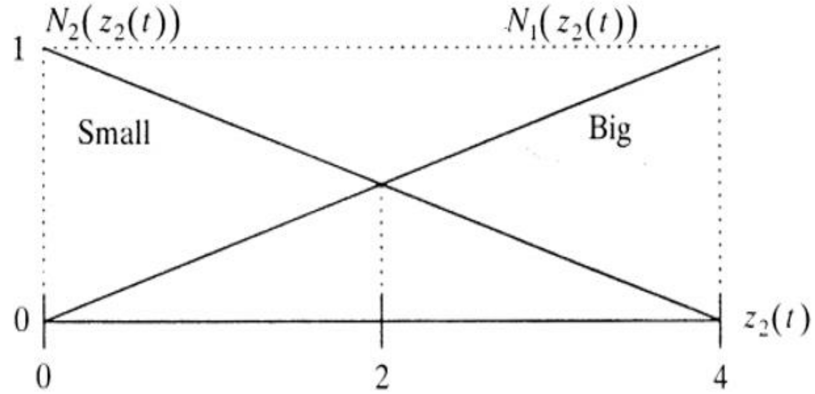

(a)- Both $M_1(z_1(t))$and $M_2(z_1(t))$ are membership functions [4].

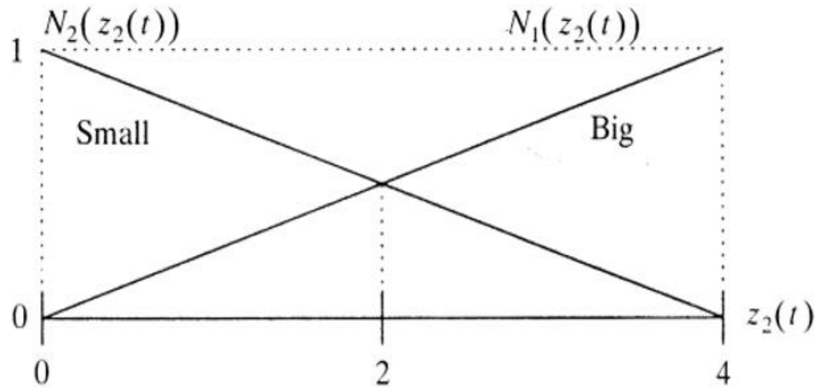

(b)- Both $N_1(z_2(t))$and $N_2(z_2(t))$ are membership functions.

Figures 2.05: Representation of the membership functions(a), (b).

The process of defuzzification is executed as

$$\dot{x}(t) = \sum_{i=1}^{4} h_i\big(z(t)\big)A_i x(t) \tag{2.44}$$

And

$$h_1 = M_1\big(z_1(t)\big) \times N_1\big(z_2(t)\big)$$

$$h_2 = M_1\big(z_1(t)\big) \times N_2\big(z_2(t)\big)$$

$$h_3 = M_2\big(z_1(t)\big) \times N_1\big(z_2(t)\big)$$

$$h_4 = M_2\big(z_1(t)\big) \times N_2\big(z_2(t)\big)$$

This fuzzy model accurately depicts the nonlinear system on the $x_1 - x_1$space in the area $[-1, 1] \times [-1, 1]$.

2.3.2.2. Parallel distributed compensation:

Kang and Sugeno (e.g., [21]) proposed a model-based design process that marked the beginning of the known as parallel distributed compensation (PDC) history. However, the design process did not address the control systems' stability. In [22], the design process was refined and the control systems' stability was examined. In [23], the design process is called "parallel distributed compensation."

From a provided T-S fuzzy model, the PDC [22, 23, 24] provides a method for designing a fuzzy controller. A T-S fuzzy model is used to depict a controlled object (nonlinear system) before the PDC is realized. We stress that a wide range of real systems, such as chaotic and mechanical systems, can and have been described using T-S fuzzy models.

Every control rule in the PDC model is derived from the matching T-S fuzzy model rule. The fuzzy model used in the premise sections and the developed fuzzy controller have the same fuzzy sets. Using the PDC, we build the fuzzy controller for the fuzzy system (2.44) as follows:

Controller Rule 1:

IF $z_1(t)$ is M_{i1} and ... and $z_p(t)$ is M_{ip}.

THEN $u(t) = -K_i(t)x(t) \qquad i = 1,2,\dots,r$

In this instance, the subsequent sections of the fuzzy control rules contain linear controller state feedback laws.

The representation of the total fuzzy controller is

$$\dot{x}(t) = \frac{\sum_{i=1}^{r} w_i\big(z(t)\big)\{A_i x(t) + B_i u(t)\}}{\sum_{i=1}^{r} w_i\big(z(t)\big)} = -\sum_{i=1}^{r} h_i\big(z(t)\big)K_i x(t) \qquad (2.45)$$

In the next sections, the design of the fuzzy controller's is used to calculate the local feedback gains K_i. PDC gives us a straightforward and organic method for managing nonlinear control systems. Additional nonlinear control methods necessitate specialized and complex understanding.

2.4. Simulation results of MVT Control for PMSM drive:

In this section, the simulation results of the proposed Model Vector Theory (MVT) control strategy applied to a Permanent Magnet Synchronous Motor (PMSM) drive are presented and analyzed. The objective of these simulations is to evaluate the effectiveness of P and PI controllers in regulating the motor speed and currents, as well as to investigate the impact of using a PWM inverter on the overall system performance.

The desired rotor speed is initially set to 50 rad/s, then increased to 150 rad/s at t = 0.25 sec. At t = 0.5 sec, the speed reference is inverted to –150 rad/s. A load torque of 5 Nm is applied at t = 0.1 sec in order to evaluate the system’s response under disturbance. The obtained results present the real and desired rotor speed, the d and q-axis stator currents, as well as the three-phase stator currents, and the load torque of the PMSM.

2.4.1. Proportional (P) controller based on MVT of PMSM:

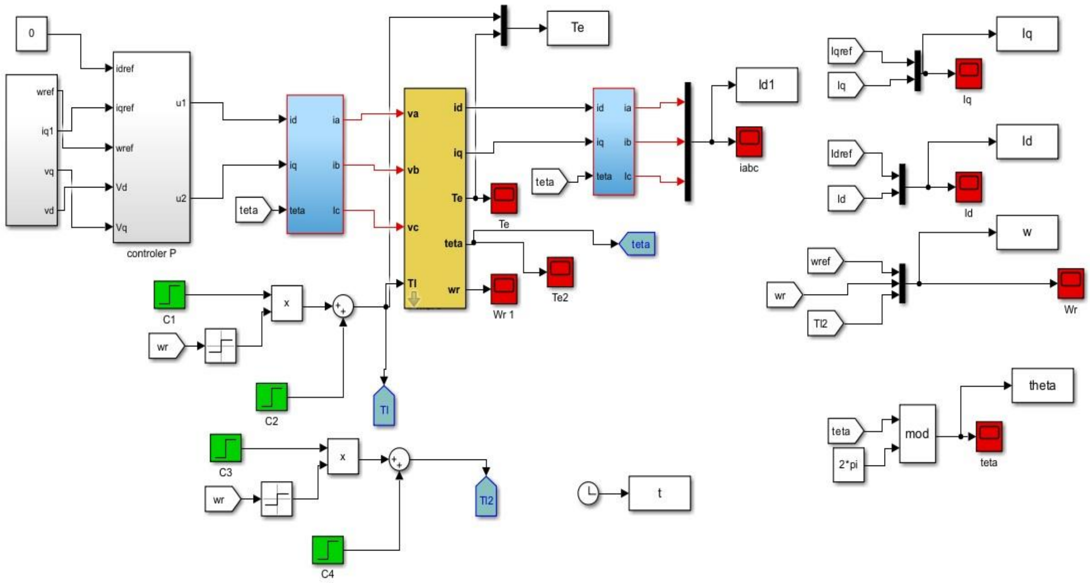

Figure 2.06: Diagram of Proportional Integral (P) controller on MVT.

The P control is applied to the PMSM without inverter and the results are shown below:

Where obtained controller gain P is:

$$K_0 = \begin{bmatrix} 0.0007 & 0 & 0.0002 \\ -0.0001 & 0.0020 & 2.0956 \end{bmatrix}$$

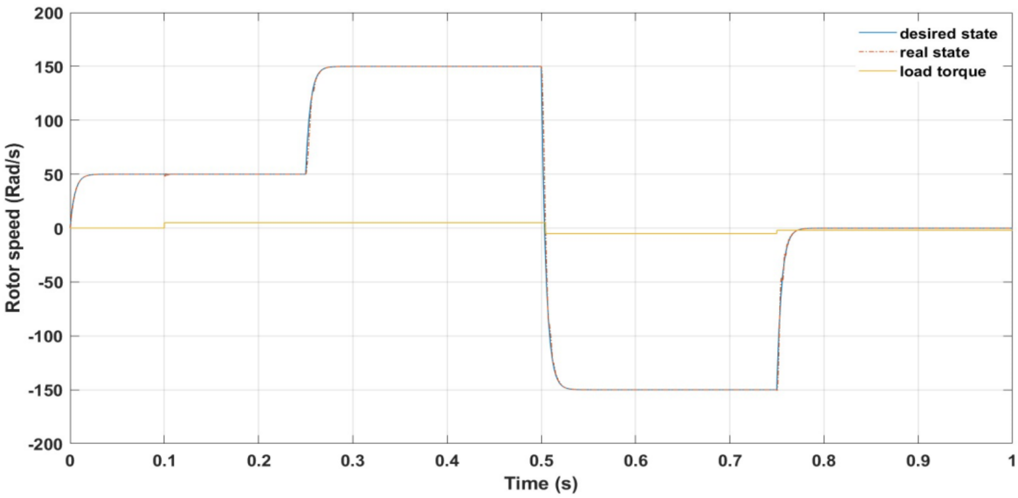

(a) Real and desired rotor speed.

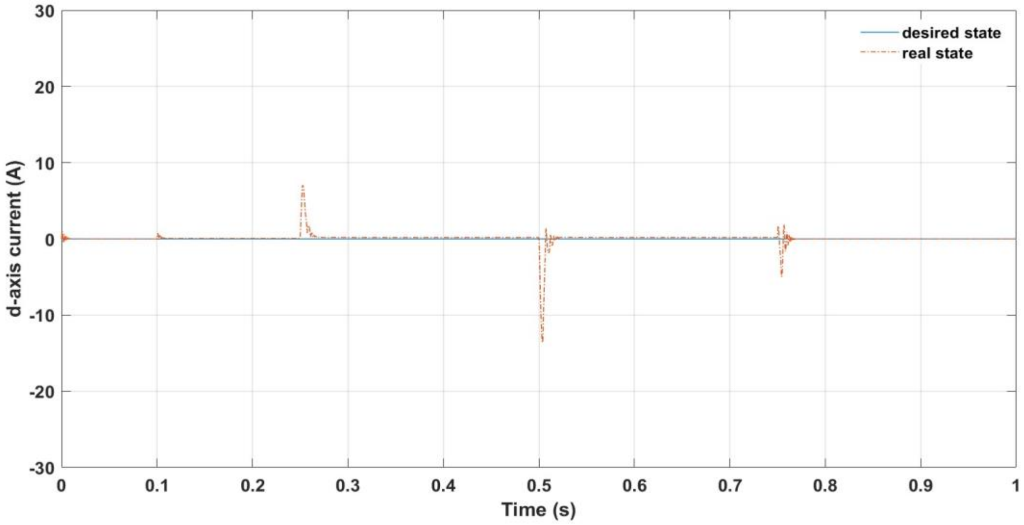

(b) Real and desired d-axis stator current.

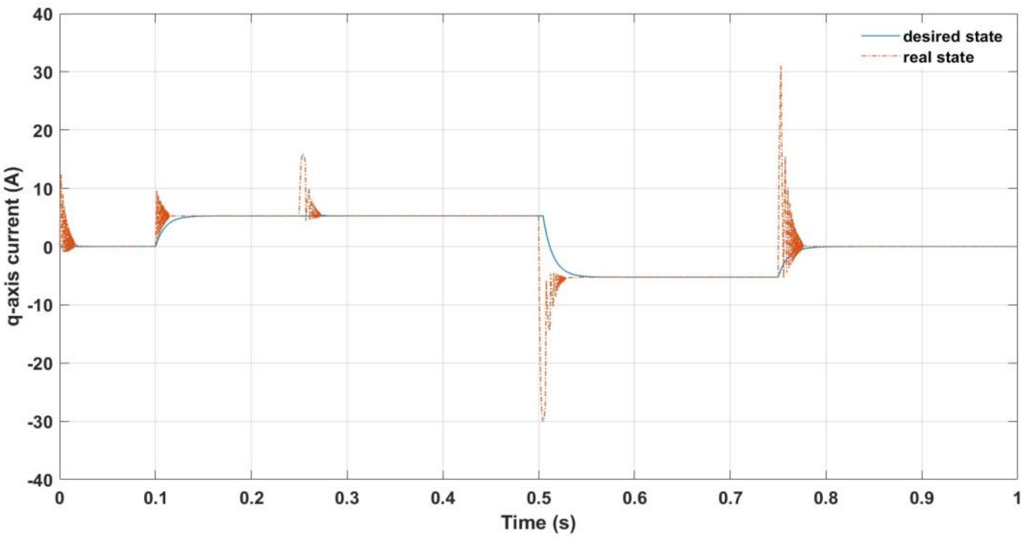

(c) Real and desired q-axis stator current.

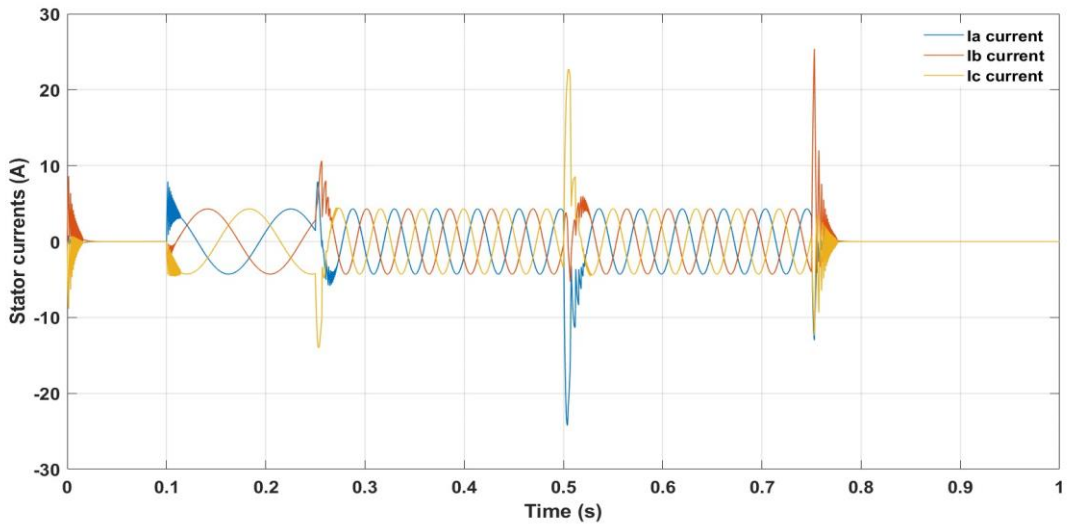

(d) Three phase stator current.

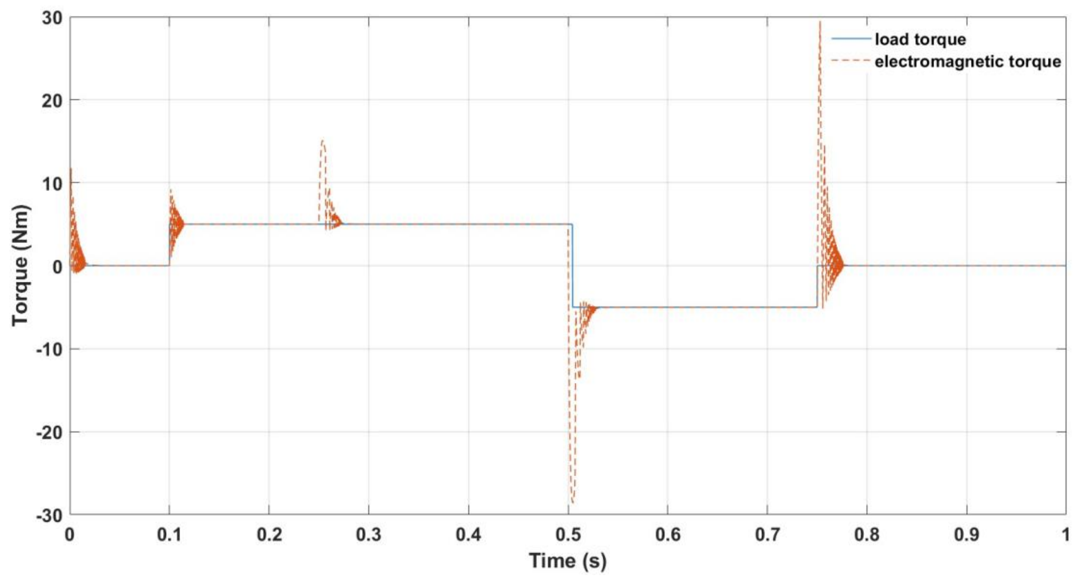

(e) Load Torque

Figure 2.07: Simulation results of P controller based on MVT Theory applied to the PMSM without PWM inverter.

2.4.2. Proportional Integral (PI) controller based on MVT of PMSM:

The proportional Integral (PI) control is applied to the PMSM without and with inverter and the results are shown below:

The obtained controller gain PI is:

$$\overline{K} = \begin{bmatrix} -0.0045 & -0.0002 & 0.0002 & 0 \\ 0.0001 & -0.0041 & 1.2259 & -0.0001 \end{bmatrix}$$

A- Without inverter:

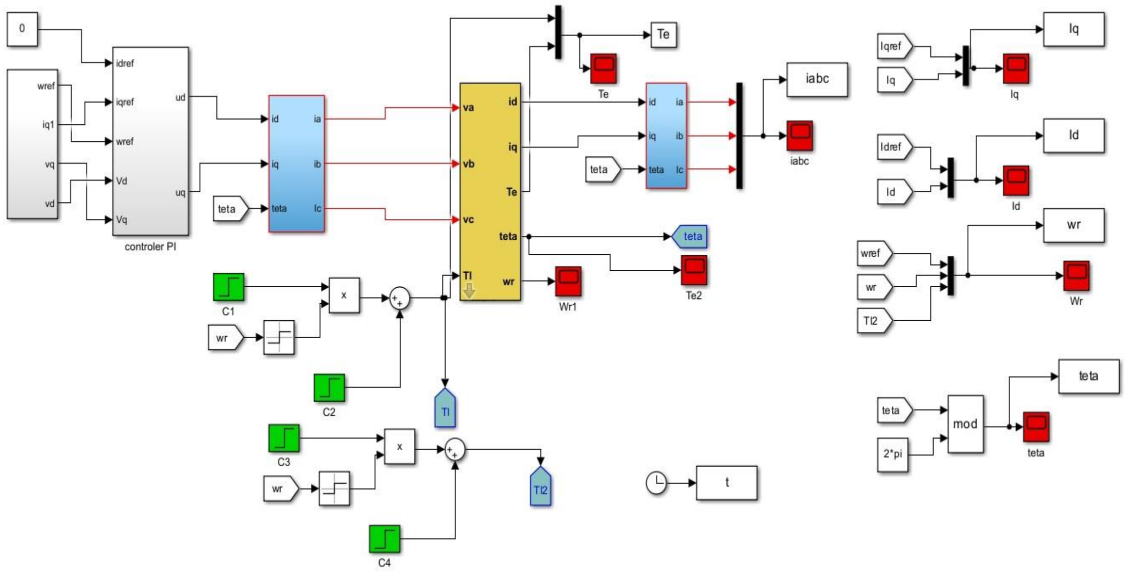

Figure 2.08: Proportional Integral (PI) controller diagram of PMSM without inverter.

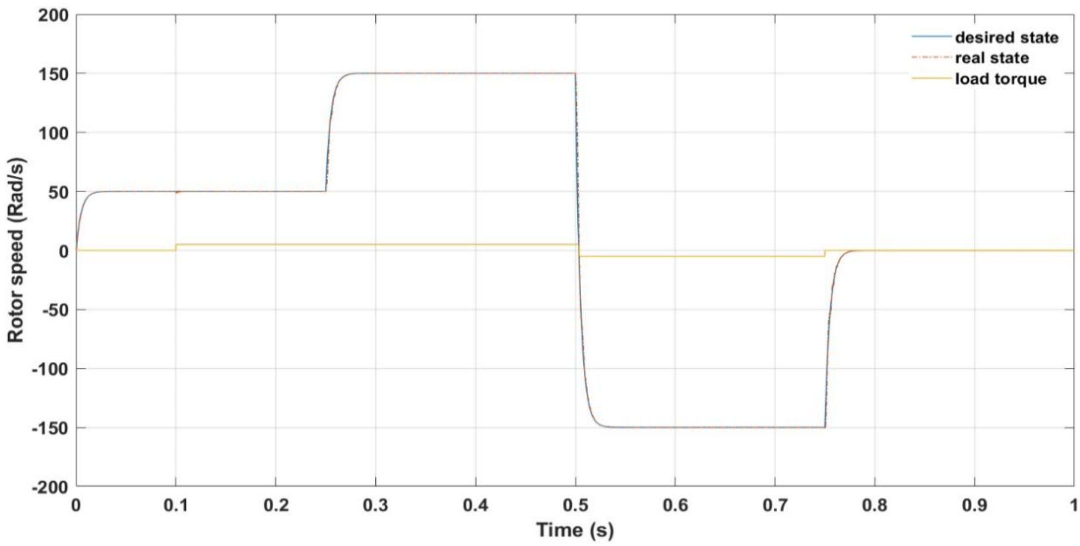

(a) Real and desired rotor speed.

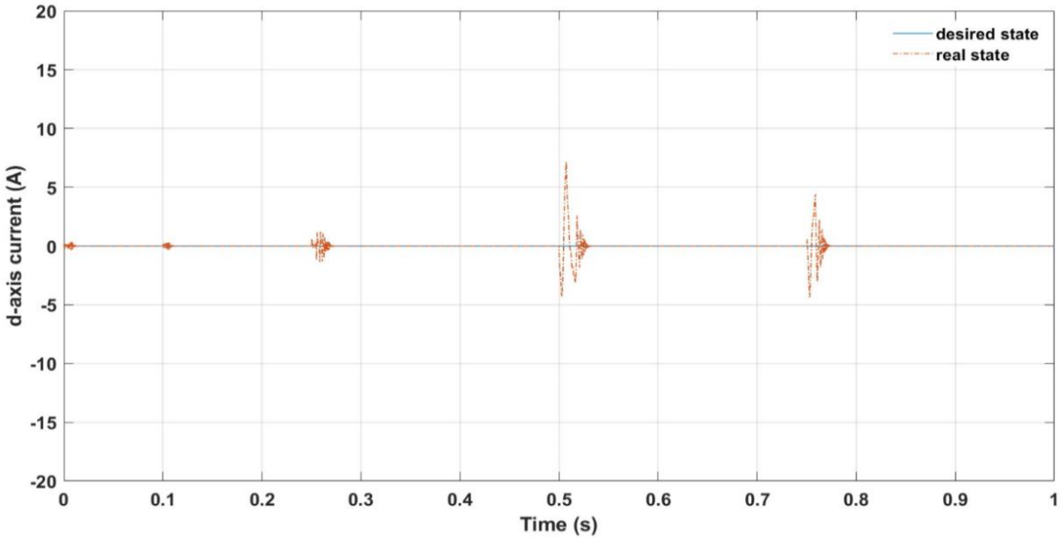

(b) Real and desired d-axis stator current.

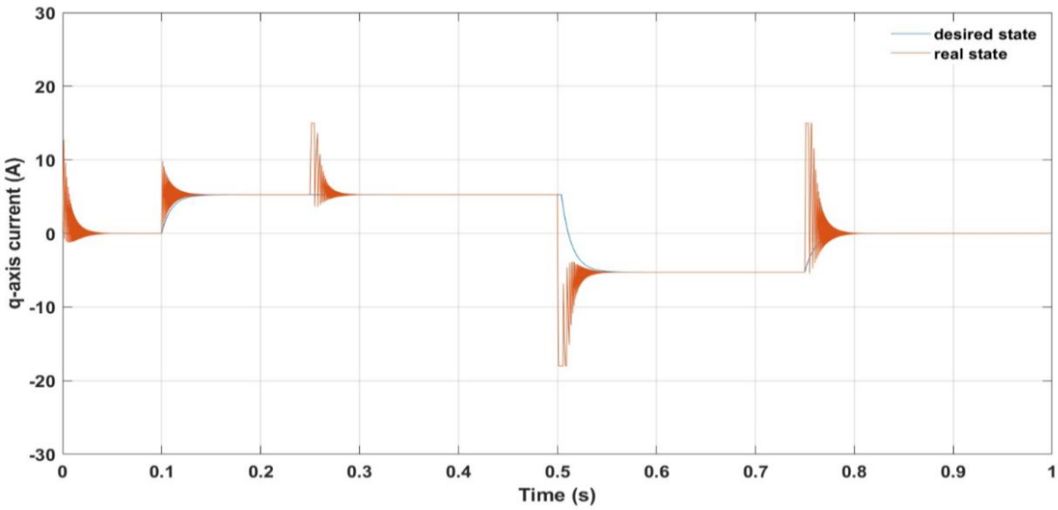

(c) Real and desired q-axis stator current.

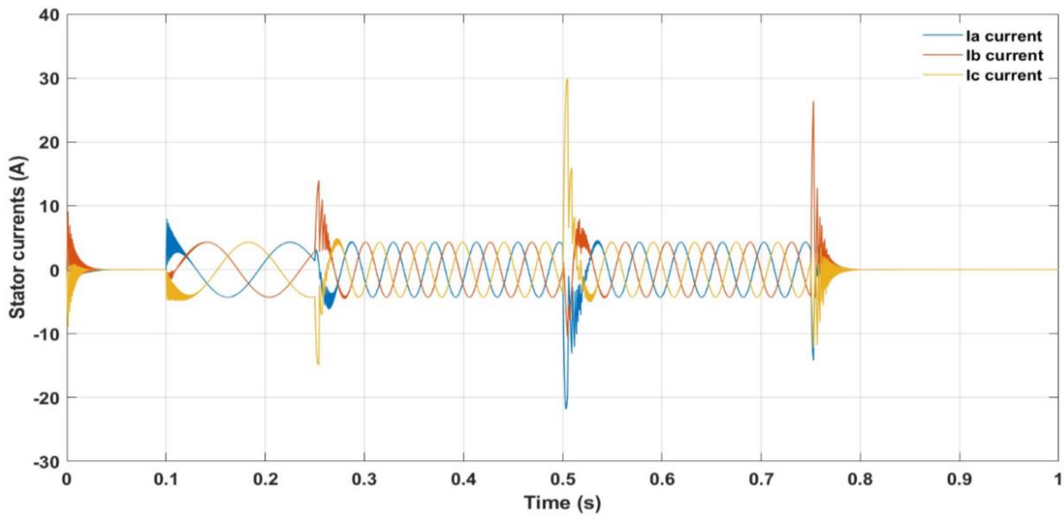

(d) Three phase stator current.

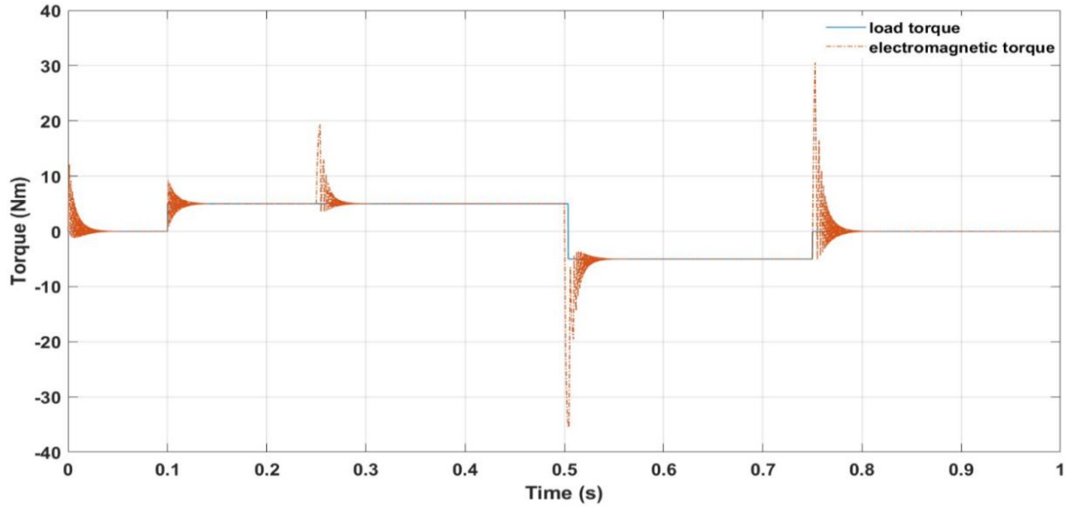

(e) Load Torque

Figure 2.09: Simulation results of PI controller based on MVT Theory applied to the PMSM without PWM inverter.

B- With inverter:

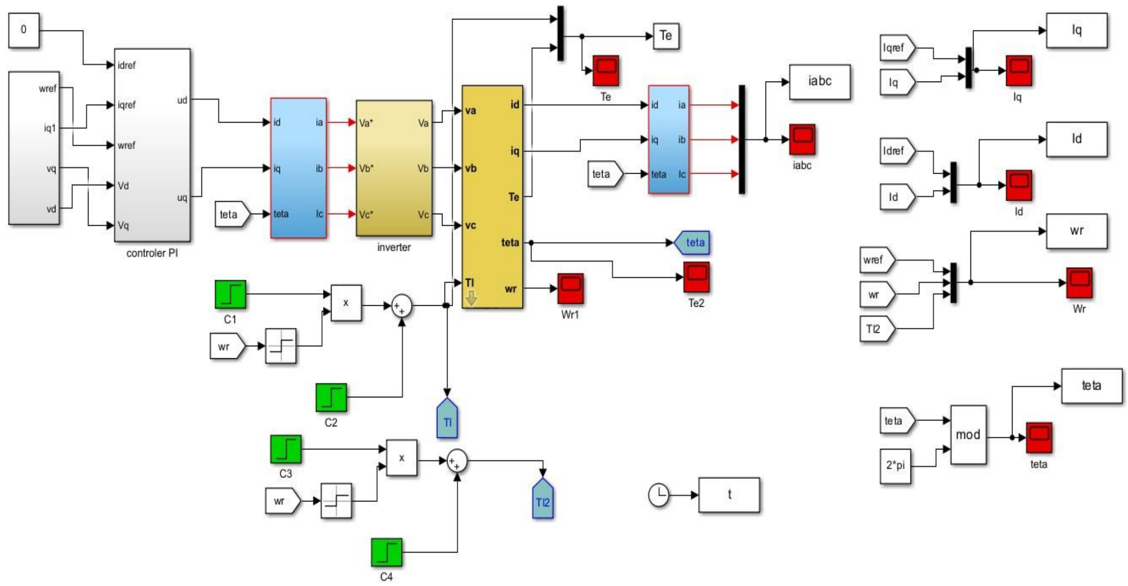

Figure 2.10: Proportional Integral (PI) controller diagram of PMSM with inverter.

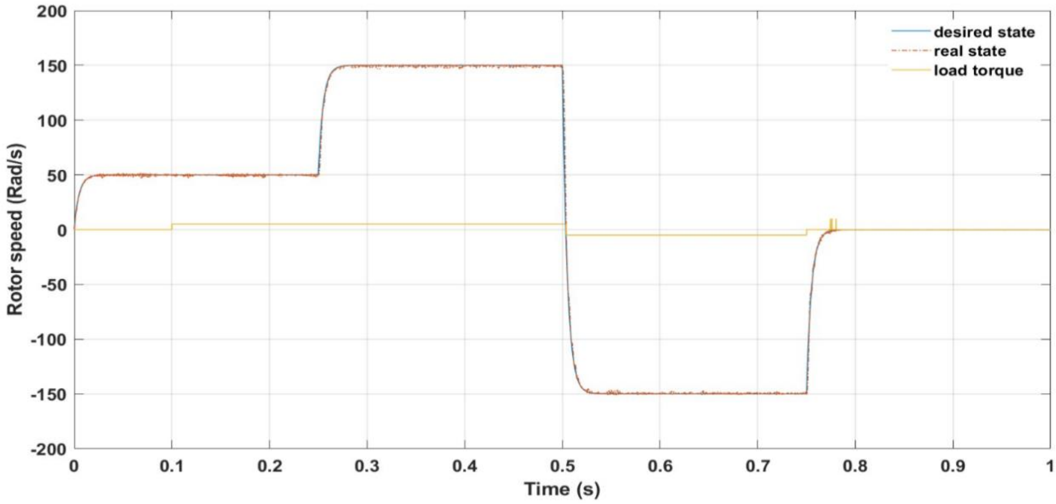

(a) Real and desired rotor speed.

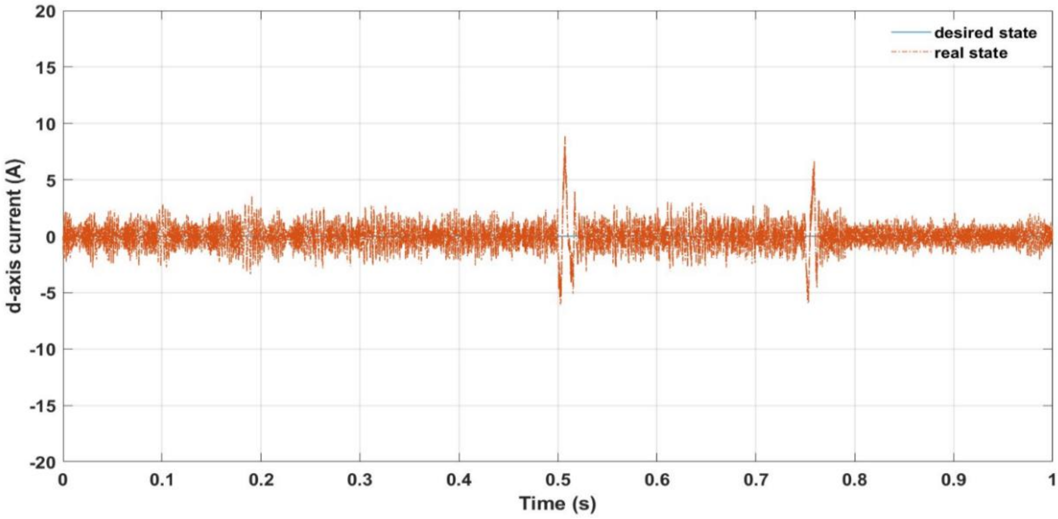

(b) Real and desired d-axis stator current.

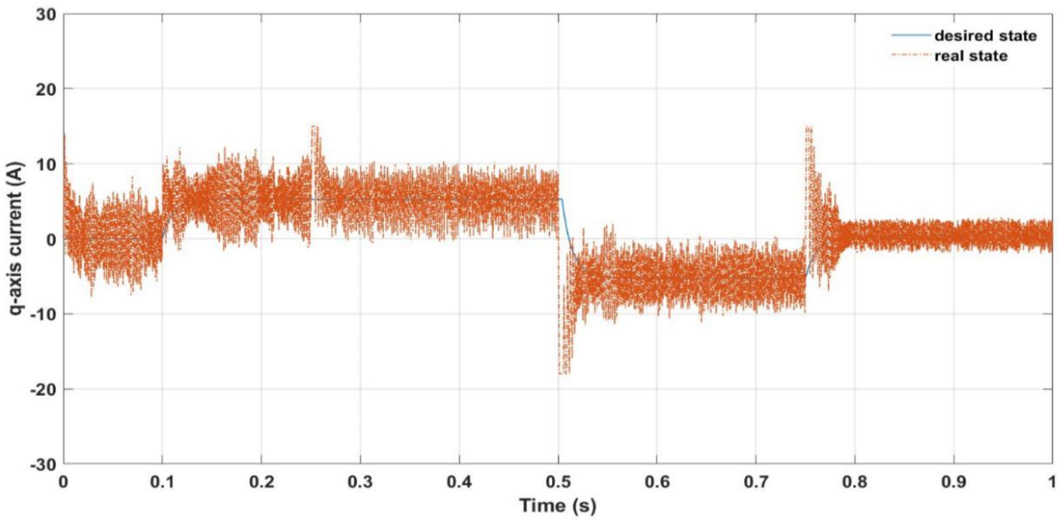

(c) Real and desired q-axis stator current.

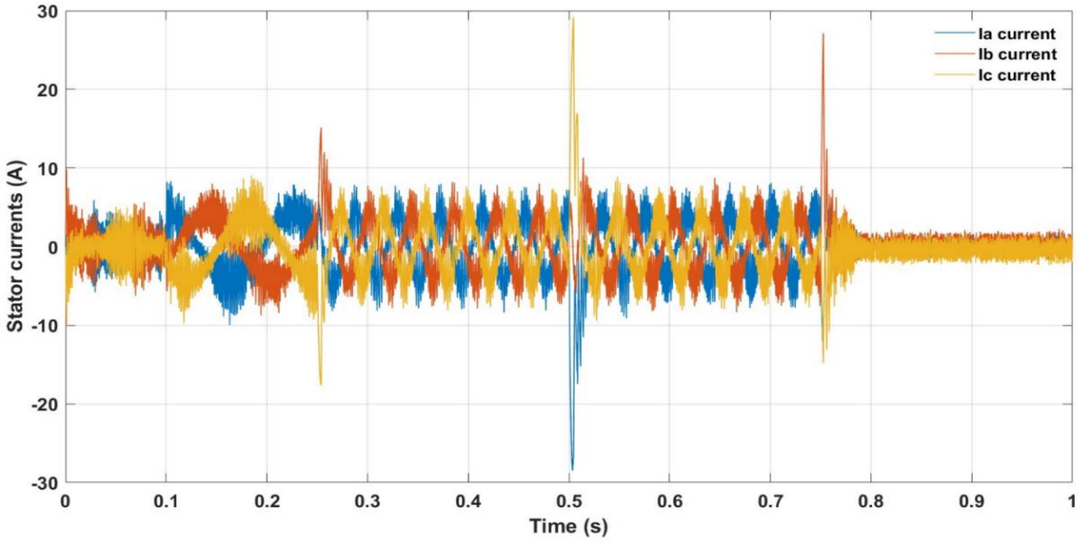

(d) Three phase stator current.

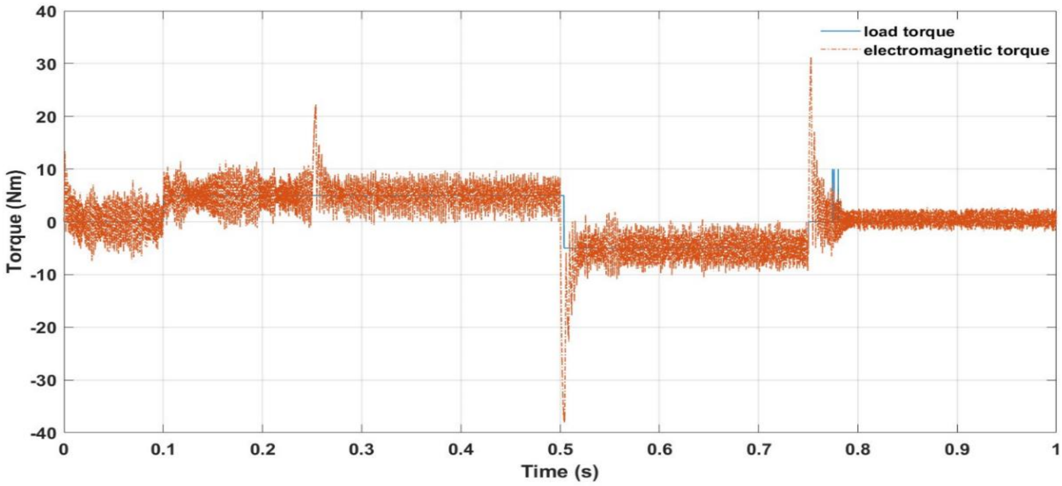

(e) Load Torque

Figure 2.11: Simulation results of PI controller based on MVT Theory applied to the PMSM with PWM inverter.

2.4.3. Simulation results discussion:

The simulation results demonstrate that the proposed MVT control is effective in regulating the PMSM drive. When comparing the use of a P controller in figure 2.07 to a PI controller in figures 2.09 and 2.11 within the MVT framework, both provide satisfactory performance, but with noticeable differences. The P controller achieves acceptable speed and current tracking; however, small steady-state errors and oscillations remain visible. By contrast, the PI controller eliminates these steady-state errors and significantly improves the quality of the responses. In particular, the PI controller ensures smoother current waveforms, more accurate tracking of the d- and q-axis currents, and reduced torque oscillations. The inclusion of the PWM inverter further enhances these results, producing highly sinusoidal three-phase currents and minimizing torque ripple. Thus, while both controllers are valid, the PI controller in combination with a PWM inverter clearly provides the best performance within the MVT control scheme.

When comparing MVT with the conventional Field-Oriented Control (FOC), the advantages of the proposed method become evident. FOC relies on coordinate transformations and precise parameter tuning to achieve current decoupling and speed regulation, which makes it more complex and sensitive to parameter variations. MVT, on the other hand, directly exploits the motor model equations, yielding faster and more robust current tracking with a simpler control structure. As a result, the MVT-controlled PMSM demonstrates smoother torque, more sinusoidal current waveforms, and superior robustness compared to FOC, all while maintaining the same fundamental objectives of accurate speed regulation and current decoupling. These results confirm that MVT is not only a feasible alternative to FOC but also a promising improvement in terms of simplicity and performance.

2.5. Conclusion:

This chapter introduced the theoretical basis of the Model Vector Theory (MVT) control for the Permanent Magnet Synchronous Motor (PMSM) and validated it through simulation results. The study confirmed that MVT achieves accurate speed regulation, effective current tracking, and smooth torque production. Both P and PI controllers were examined, and while each ensured satisfactory performance, the PI controller combined with a PWM inverter provided the most accurate and stable results. Compared to conventional Field-Oriented Control (FOC), the MVT method proved to be simpler, less dependent on parameter tuning, and capable of delivering equal or superior performance.

However, the simulations presented in this chapter were performed under ideal operating conditions without considering external disturbances or parameter variations. In practice, PMSM drives are often subject to load disturbances, measurement noise, and model uncertainties, which may affect control performance.For this reason, the next chapter is dedicated to the design of the MVT control strategy for PMSM under disturbances.

The last Chapter will focus on enhancing the robustness of the proposed method, ensuring stable and reliable operation even in the presence of uncertainties and external perturbations.

2.6. References:

[1] Baranyi P. TP model transformation as a way to LMI-basedcontroller design. IEEE Transactions on Industrial Electronics,2004, 51(2): 387–400

[2] Merzoug M., Naceri F., “Comparison of field-oriented control and direct torque control for permanent magnet synchronous motor (PMSM),” International Journal of Electrical, Computer, Energetic, Electronics and Communication Engineering, vol. 2, no. 9, pp. 107–112, 2008.

[3] Molavi R., Khaburi D. A., “Optimal control strategies for speed control of permanent-magnet synchronous motor drives,” World Academy of Science, Engineering and Technology, vol. 2, no. 8, pp. 288–292, 2008.

[6] Štulrajter M., Hrabovcová V., Franko M., “Permanent magnets synchronous motor control theory,” Journal of Electrical Engineering, vol. 58, no. 2, pp. 79–84, 2007.

[7] Novotny D., Lipo T., Vector Control and Dynamics of AC Drives, Oxford University Press, 1996.

[6] Solsona J., Valla M. I., Muravchik C., “Nonlinear control of a permanent magnet synchronous motor with disturbance torque estimation,” IEEE Transactions on Energy Conversion, vol. 15, no. 2, pp. 163–168, 2000.

[7] Shi J. L., Liu T. H., Chang Y. C., “Optimal controller design of a sensorless PMSM control system,” 31st Annual Conference of IEEE Industrial Electronics Society (IECON), 2005

.

[8] Zemouche A., Boutayeb M., Bara G. I., “Observers for a class of Lipschitz systems with extension to H∞ performance analysis,” Systems & Control Letters, vol. 57, no. 1, pp. 18–27, 2008.

[9] Sahoo P. K., Riedel T., Mean Value Theorems and Functional Equations, World Scientific Publishing Company, 1999.

[10] Ichalal D, Arioui H, Mammar S. Observer design for two-wheeledvehicle: a Takagi-Sugeno approach with unmeasurable premisevariables. In: Proceedings of the 19th Mediterranean Conference onControl and Automation. Corfu, Greece, 2011, 1–6

[11] Bergsten P., Palm R., Driankov D., “Observers for Takagi-Sugeno fuzzy systems,” IEEE Transactions on Systems, Man, and Cybernetics – Part B: Cybernetics, vol. 32, no. 1, pp. 114–121, 2002.

[12] Bara G I, Daafouz J, Kratz F, Ragot J. Parameter dependent stateobserver design for affine LPV systems. International Journal ofControl, 2001, 74(16): 1601–1611

[13] Zemouche A, Boutayeb M, Bara G I. Observer design for nonlinearsystems: an approach based on the differential mean value theorem. In: Proceedings of the 44th IEEE Conference on Decision andControl. Seville, Spain, 2005, 6353–6358

[14] Tanaka K, Wang H O. Fuzzy Control Systems Design and Analysis:A Linear Matrix Inequality Approach. Wiley-Interscience, 2001

[15] Raghavan S., Hedrick J. K., “Observer design for a class of nonlinear systems,” International Journal of Control, vol. 59, no. 2, pp. 515–528, 1994.

[16] Tanaka K., Wang H. O., Fuzzy Control Systems Design and Analysis: A Linear Matrix Inequality Approach, John Wiley & Sons, 2004.

[17] Takagi T., Sugeno M., “Fuzzy identification of systems and its applications to modeling and control,” in Readings in Fuzzy Sets for Intelligent Systems, Elsevier, 1993, pp. 387–403.

[18] Sugeno M., Kang G., “ Structure identification of fuzzy model, ” Fuzzy Sets and Systems, vol. 28, pp. 15–33, 1988.

[19] Sugeno M., Fuzzy Control, Nikkan Kougyou Shinbunsha Publisher, Tokyo, 1988.

[20] Sugeno M., Kang G., “Fuzzy modelling and control of multilayer incinerator,” Fuzzy Sets and Systems, vol. 18, pp. 329–345, 1986.

[21] Tanaka K., Sugeno M., “Stability analysis and design of fuzzy control systems,” Fuzzy Sets and Systems, vol. 45, pp. 135–156, 1992.

[22] Wang H. O., Tanaka K., Griffin M., “Parallel distributed compensation of nonlinear systems by Takagi-Sugeno fuzzy model,” in Proceedings of 1995 IEEE International Conference on Fuzzy Systems, 1995, pp. 531–538.

[23] Wang H. O., Tanaka K., Griffin M., “An analytical framework of fuzzy modeling and control of nonlinear systems: stability and design issues,” in Proceedings of 1995 American Control Conference (ACC’95), 1995, pp. 2272–2276.

[24] H. O. Wang, K. Tanaka, and M. Griffin, "An analytical framework of fuzzy modeling andcontrol of nonlinear systems: stability and design issues," in Proceedings of 1995 American Control Conference-ACC'95, 1995, pp. 2272-2276.

Chapter 03
Robust PI-MVT H∞ controller

3.1. Introduction:

PMSM machines have garnered a lot of attention for use in industrial drive applications. PMSM is a good alternative in many applications because of its many advantages over asynchronous motor drives, including high efficiency [1], compact structure, high air-gap flux density, high torque to weight ratio [2, 3], high torque density, and simpler controller. In the industry, Direct Torque Control (DTC) and Field-Oriented Control (FOC) techniques have been used with effectiveness. The goal is to efficiently regulate the motor torque and flux in order to compel the motor to follow the trajectory exactly, irrespective of changes in the load parameters and machine or any unrelated disruptions [4, 5]. Nevertheless, PMSMs are dynamic, non-linear multivariable systems, and their electrical properties change as the temperature rises.

Using the mean value theorem (MVT), we attempt in this chapter to develop a classical feedback control in H_∞ performance that ensures stability and rejection of disturbances.

We make the assumption that every state variable is accessible for feedback. There have been a number of presentations on feedback control design [6–7]. The author discusses approaches that use model linearization around a working point in order to apply linear control theory in chapters [8–9]. This solution limited the feedback controller's effectiveness. The Takagi-sugeno model (PDC) fuzzy controller design is discussed in [10–11]. Despite the PDC approach's success, there are a number of drawbacks, including the controller's dependence on the system states.

3.2. Controller design:

3.2.1. A physical model of PMSM:

Voltage equations provide the dynamic model that was taken from the rotor reference:

$$\begin{cases} u_d = R_s I_d + \dfrac{d\lambda_d}{dt} + p\Omega\lambda_q \\ u_q = R_s I_q + \dfrac{d\lambda_q}{dt} + p\lambda_d \end{cases} \tag{3.01}$$

Where $\lambda_d = \lambda_{pm} + L_d I_d$; $\lambda_q = L_q I_q$

The following equations can be used to represent an N-L model of PMSM:

$$\begin{cases} \dfrac{dI_d}{dt} = -\dfrac{R_s}{L_d} I_d + \dfrac{L_q}{L_d} p\Omega + \dfrac{1}{L_d} u_d \\ \dfrac{dI_q}{dt} = -\dfrac{R_s}{L_q} I_q - \dfrac{L_d}{L_q} p\Omega I_d + \dfrac{\lambda_{pm}}{L_q} p\Omega + \dfrac{1}{L_q} u_q \\ \dfrac{d\Omega}{dt} = \dfrac{1}{J}(T_e - T_L - f\Omega) \end{cases} \tag{3.02}$$

The motor torque is expressed by:

$$T_e = \frac{3}{2} p\left[\left(L_d - L_q\right) I_d I_q + \lambda_{pm} I_q\right] \tag{3.03}$$

From (3.02) and (3.03), we can rewrite the state model as:

$$\begin{cases} \dot{x}(t) = f\big(x(t)\big) + Bu(t) + Dw(t) \\ y(t) = Cx(t) \end{cases} \tag{3.04}$$

And

$$f(x) = \begin{bmatrix} a_1 x_1 + a_2 x_3 x_2 \\ b_1 x_2 + b_2 x_1 x_3 + b_3 x_3 \\ c_1 x_1 x_2 + c_2 x_2 + c_3 x_3 \end{bmatrix};$$

$$B = \begin{bmatrix} \lambda_d & 0 \\ 0 & \lambda_q \\ 0 & 0 \end{bmatrix}; \quad D = \begin{bmatrix} 0 \\ 0 \\ c_4 \end{bmatrix} \tag{3.05}$$

Where

$x = [x_1 \;\; x_2 \;\; x_3]^T = [i_d \;\; i_q \;\; \Omega]^T$, $u = [u_d \quad u_q]^T$, $w = T_L$

$$a_1 = -\frac{R_s}{L_d}, \quad a_2 = \frac{L_q}{L_d} p, \quad b_1 = -\frac{R_s}{L_q},$$

$$b_2 = -\frac{L_d}{L_q} p, \quad b_3 = \frac{\lambda_{pm}}{L_q} p,$$

$$c_1 = \frac{3p}{2J}\left(L_d - L_q\right), \quad c_2 = \frac{3p}{2J}\lambda_{pm}, \quad c_3 = -\frac{f}{J}, \quad c_4 = -\frac{1}{J},$$

$$\lambda_d = \frac{1}{L_d}, \quad \lambda_q = \frac{1}{L_q},$$

3.2.2. Problem statemant:

This section presents a successful approach to controller design for the category of nonlinear systems (3.04) as defined by:

$$\begin{cases} \dot{x}(t) = A_0x(t) + B_0u(t) + \Phi(x) + Dw(t) \\ y(t) = Cx(t) \end{cases} \qquad (3.06)$$

The state vector $x \in R^n$, input vector $u \in R^p$, output measurement vector $y \in R^m$, disturbance vector $w \in R^q$, and $C \in R^{n\times m}$ and $D \in R^{n\times q}$ are suitable matrix. The function: $\Phi(x)\; R^n \to R^n$ are nonlinear. $\Phi(x)$ are also thought to be differentiable. And A_0, B_0 are acquired as follows using the Takagi-Sugeno model:

$$A_0 = \frac{1}{r}\sum_{i=1}^{r} A_i \; ; \quad B_0 = \frac{1}{r}\sum_{i=1}^{r} B_i \; ; \quad \bar{A}_i = A_i - A_0 \; ;$$

$$\bar{B}_i = B_i - B_0$$

Where

$$\Phi(x) = \sum_{i=1}^{r} \mu_i(x)(\bar{A}_i x + \bar{B}_i u)$$

3.2.3. State feedback control:

The form of the feedback command under discussion is similar to that of classical design.

$$u(t) = -K_0 e(t) \qquad (3.07)$$

where the error's state vector:

$$e(t) = x(t) - x_c(t) \qquad (3.08)$$

K_0 is the controller's gain, and $x_c = [i_{dc} \;\; i_{qc} \;\; \Omega_c]^T$ is the desired state. The signal is meant to be stepwise. The goal is to identify the gain matrix K_0 at which the nonlinear system (3.06) achieves asymptotic stability.

The closed-loop error state dynamic equation can be derived using equations (3.06) and (3.07) as follows:

$$\dot{e}(t) = \dot{x}(t) - \dot{x}_c(t) \qquad (3.09)$$

$$\dot{e}(t) = \dot{x}(t) = (A_0 - B_0K_0)e(t) + \{\Phi(x) - \Phi(x_c)\} + Dw(t) \\ +A_0x_c + \Phi(x_c) \tag{3.10}$$

Keep in mind that it is not possible to directly reach the stability analysis of it. In conclusion, the goal is to determine the gain matrix K_0 that stabilizes equation.

The solution for the suggested controller design is to acquire an adequate form of the state controller error. The MVT and sector nonlinear transformation must be added prior to the controller's synthesis.

Adding an integral action is preferred in order to remove the perturbation impacts and parametric steady-state uncertainties. The new control law then states:

$$u(t) = -[K_0 \quad K_I]\begin{bmatrix} e(t) \\ e_I(t) \end{bmatrix} = \bar{K}\bar{e}(t) \tag{3.11}$$

Such as the state related to integral action:

$$\dot{e}_I(t) = x(t) - x_c(t) \tag{3.12}$$

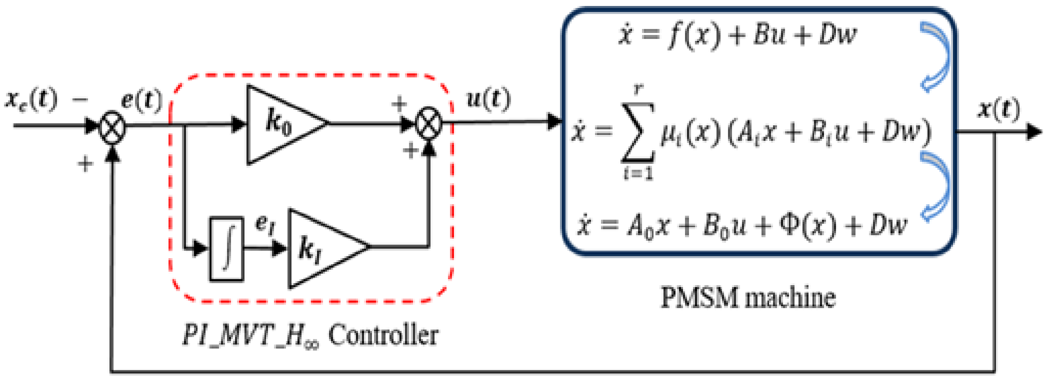

Figure 3.01: The control strategy of PI-MVT H∞ controller for PMSM.

Figure 3.01 shows a control strategy based on the MVT theorem and h performance that uses an integral action.

3.2.4. LMI formulation for H_∞ performance:

The H_∞ of the transfer $\boldsymbol{T}_\infty$ between $w(t)$ and $e(t)$ is:

$$\|T_{ew}\|_\infty = sup_{\|w(t)\|_2 \neq 0} \frac{\|e(t)\|_2^2}{\|w(t)\|_2^2} \tag{3.13}$$

Where

$$\|w(t)\|_2^2 = \int_0^\infty \sigma^T(t)\,\sigma(t)\,dt \tag{3.14}$$

The goal is to identify a control rule that reduces the transfer between $\overline{w}(t)$ and $\bar{e}(t)$ so that $\|T_{\bar{e}\overline{w}}\|_\infty < \gamma$ and γ equals the rate of mitigation, so attenuating the effect of external disturbances $\overline{w}(t)$ on the quantity to be stabilized $\bar{e}(t)$. Criterion H_∞ in this instance can be reformulated as

$$\int_0^\infty \bar{e}^T(t)\,\bar{e}(t)\,dt \leq \gamma^2 \int_0^\infty \overline{w}^T(t)\,\overline{w}(t)\,dt \tag{3.15}$$

Lemma 01:

If there are matrices, like $X = X^T > 0$, then the closed-loop system's quadratic stability is ensured for an attenuation of the external disturbances $\mathrm{w}(t)$ based on the rate $\delta = \gamma^2$.

$$Q_i = \begin{bmatrix} \bar{A}_i X + X\bar{A}_i{}^T - \bar{B}Y - Y^T\bar{B}^T & \overline{D}_w & X \\ \overline{D}_w{}^T & -\gamma^2 I & 0 \\ X & 0 & I \end{bmatrix} < 0 \tag{3.16}$$

gain $\overline{K}$ is found by:

$$\overline{K} = YX^{-1}$$

the quadratic function of Lyapunov provided by:

$$V(\bar{e}(t)) = \bar{e}^T(t)P\bar{e}(t) \tag{3.17}$$

Under the performance H_∞, the stablility in the case of the quadratic Lyapunov candidate function (3.17).

$$\dot{V}(\bar{e}(t)) + \bar{e}^T(t)\bar{e}(t) - \gamma^2\overline{w}^T(t)\overline{w}(t) < 0 \tag{3.18}$$

We Replace the derivative of $V(\bar{e}(t))$ in:

$$\dot{\bar{e}}^T(t)P\bar{e}(t) + \bar{e}^T(t)P\dot{\bar{e}}(t) + \bar{e}^T(t)\bar{e}(t) - \gamma^2\bar{w}^T(t)\bar{w}(t) < 0 \tag{3.19}$$

Else:

$$\begin{aligned}&\sum_{i=1}^{r}\mu_i(x(t))\,\bar{e}^T(t)\left[\bar{G}_i{}^T P + P\bar{G}_i\right]\bar{e}(t) + \sum_{i=1}^{r}\mu_i(x(t))\,\bar{w}^T(t)\left[\bar{D}_w{}^T P\right]\bar{e}(t)\\ &\quad + \sum_{i=1}^{r}\mu_i(x(t))\,\bar{e}^T(t)[P\bar{D}_w]\bar{w}(t) - \gamma^2\bar{w}^T(t)\bar{w}(t) < 0\end{aligned} \tag{3.20}$$

The inequality (3.20) is expressed in the vector notation:

$$\sum_{i=1}^{r}\mu_i(x(t))\,[\bar{e}^T(t) \quad \bar{w}^T(t)]\begin{bmatrix}\bar{G}_i{}^T P + P\bar{G}_i + I & P\bar{D}_w\\ \bar{D}_w{}^T P & -\gamma^2 I\end{bmatrix}\begin{bmatrix}\bar{e}(t)\\ \bar{w}(t)\end{bmatrix} < 0 \tag{3.21}$$

Or

$$\begin{bmatrix}\sum_{i=1}^{r}\mu_i(x(t))\left[\bar{G}_i{}^T P + P\bar{G}_i\right] + I & P\sum_{i=1}^{r}\mu_i(x(t))\,\bar{D}_w\\ \sum_{i=1}^{r}\mu_i(x(t))\,\bar{D}_w{}^T P & -\gamma^2 I\end{bmatrix} < 0 \tag{3.22}$$

$$\begin{bmatrix}\sum_{i=1}^{r}\mu_i(x(t))\left[\bar{G}_i{}^T P + P\bar{G}_i\right] & P\sum_{i=1}^{r}\mu_i(x(t))\,\bar{D}_w\\ \sum_{i=1}^{r}\mu_i(x(t))\,\bar{D}_w{}^T P & -\gamma^2 I\end{bmatrix}\begin{bmatrix}I & 0\\ 0 & 0\end{bmatrix} < 0 \tag{3.23}$$

$$\begin{bmatrix}\sum_{i=1}^{r}\mu_i(x(t))\left[\bar{G}_i{}^T P + P\bar{G}_i\right] & P\sum_{i=1}^{r}\mu_i(x(t))\,\bar{D}_w\\ \sum_{i=1}^{r}\mu_i(x(t))\,\bar{D}_w{}^T P & -\gamma^2 I\end{bmatrix}\begin{bmatrix}I\\ 0\end{bmatrix}[I \quad 0] < 0 \tag{3.24}$$

we get:

$$\begin{bmatrix} \sum_{i=1}^{r} \mu_i(x(t)) \left[\bar{G}_i^{\ T} P + P\bar{G}_i\right] & P\sum_{i=1}^{r} \mu_i(x(t))\,\bar{D}_w & I \\ \sum_{i=1}^{r} \mu_i(x(t))\,\bar{D}_w^{\ T} P & -\gamma^2 I & 0 \\ I & 0 & -I \end{bmatrix} < 0 \tag{3.25}$$

$$\sum_{i=1}^{r} \mu_i(x(t)) \begin{bmatrix} \bar{G}_i^{\ T} P + P\bar{G}_i & P\bar{D}_w & I \\ \bar{D}_w^{\ T} P & -\gamma^2 I & 0 \\ I & 0 & -I \end{bmatrix} < 0 \tag{3.26}$$

The (3.26) inequalities are nonlinear. By applying the congruence transformation and multiplying them by the diagonal matrix $[P^{-1}, \ \ I, \ \ I]$ on the right and left, we may create them LMI.

$$\begin{bmatrix} P^{-1} & 0 & 0 \\ 0 & I & 0 \\ 0 & 0 & I \end{bmatrix} \begin{bmatrix} \bar{G}_i^{\ T} P + P\bar{G}_i & P\bar{D}_w & I \\ \bar{D}_w^{\ T} P & -\gamma^2 I & 0 \\ I & 0 & -I \end{bmatrix} \begin{bmatrix} P^{-1} & 0 & 0 \\ 0 & I & 0 \\ 0 & 0 & I \end{bmatrix} < 0 \tag{3.27}$$

After development, the expression (3.27) is rewritten:

$$\begin{bmatrix} P^{-1}\left[\bar{G}_i^{\ T} P + P\bar{G}_i\right] P^{-1} & P^{-1} P\bar{D}_w & P^{-1} \\ \bar{D}_w^{\ T} P P^{-1} & -\gamma^2 I & 0 \\ P^{-1} & 0 & -I \end{bmatrix} < 0 \tag{3.28}$$

Using the change of variables $X^{-1} = P$ et $Y = \bar{K}P^{-1} = \bar{K}X$, we obtain the following expression:

$$\begin{bmatrix} \bar{A}_i X + X\bar{A}_i^{\ T} - \bar{B}Y - Y^T \bar{B}^T & \bar{D}_w & X \\ \bar{D}_w^{\ T} & -\gamma^2 I & 0 \\ X & 0 & -I \end{bmatrix} < 0 \tag{3.29}$$

In the case of the proportional regulator $P\_MVT\_H_\infty$ the LMI can be reduced to:

$$\begin{bmatrix} A_i N + N A_i^{\ T} - BM - M^T B^T & D_w & N \\ D_w^{\ T} & -\gamma^2 I & 0 \\ N & 0 & -I \end{bmatrix} < 0 \tag{3.30}$$

For instance, $K_0 = MN^{-1}$ is used to determine the gain K_0. The LMI issue presented by (3.29) and (3.30), respectively, is solved to determine the gain K_0 and $\overline{K}$ of the $P/PI\_MVT\_H_\infty$ that which ensures the exponential convergence.

3.3. Conclusion:

In this chapter, the design methodology of the PI–MVT–H∞ controller for Permanent Magnet Synchronous Motor (PMSM) drives has been presented. The proposed control structure integrates three complementary techniques: the proportional–integral (PI) controller for steady-state regulation, the Mean Value Theorem (MVT) approach for managing system nonlinearities through a Linear Parameter Varying (LPV) representation, and the H∞ robust control framework to ensure stability margins and disturbance rejection in the presence of uncertainties.

The design process established the theoretical foundations required to synthesize this hybrid controller, highlighting its advantages over classical control strategies. By combining the simplicity of PI regulation with the robustness of H∞ optimization and the nonlinear system handling capability of the MVT approach, the proposed architecture provides a balanced and effective solution for PMSM control.

Although no simulation or experimental results were provided in this chapter, the controller design represents a significant contribution to the field. It establishes a robust theoretical framework upon which future implementations and validations can be carried out. The proposed PI–MVT–H∞ controller is expected to outperform conventional PI and sliding mode controllers, offering better robustness, stability, and precision in demanding industrial and automotive appications. In this chapter concludes the methodological contributions of the thesis, setting the stage for future work where the designed controller can be simulated, implemented, and experimentally validated in practical PMSM drive systems.

3.4. References:

[1] M. Bodson, J. Chiasson, and R. Novotnak, "High-performance induction motor control via input-output linearization," *IEEE control systems,* vol. 14, no. 4, pp. 25-33, 1994.

[2] R. Molavi, and D. Khaburi, "Optimal control strategies for speed control of permanent-magnet synchronous motor drives." pp. 428-432.

[3] C.-T. Pan, and J.-H. Liaw, "A robust field-weakening control strategy for surface-mounted permanent-magnet motor drives," *IEEE Transactions on Energy Conversion,* vol. 20, no. 4, pp. 701-709, 2005.

[4] M. Merzoug, and F. Naceri, "Comparison of field-oriented control and direct torque control for permanent magnet synchronous motor (pmsm)." pp. 299-304.

[5] M. Štulrajter, V. Hrabovcova, and M. Franko, "Permanent magnets synchronous motor control theory," *Journal of Electrical Engineering,* vol. 58, no. 2, pp. 79-84, 2007.

[6] L. ZHANG, D. LI, Y. XUE, and D. TANG, "PID controller design for H_∞ mixed sensitivity restriction [J]," *Journal of Tsinghua University (Science and Technology),* vol. 5, pp. 032, 2005.

[7] N. Zhao, and B.-m. Ge, "H∞ robust control of permanent magnet synchronous motor used in electric vehicle [J]," *Electric machines and control,* vol. 5, pp. 007, 2007.

[8] C. Duval, G. Clerc, and Y. Le Gorrec, "Induction machine control using robust eigenstructure assignment," *Control Engineering Practice,* vol. 14, no. 1, pp. 29-43, 2006.

[9] B. Hamidani, A. Allag, O. Zeghib, and A. Allag, "An extended observer based-controller applied to sensorless PMSM drive using the mean value theorem and Lipchitz models," *International Journal of System Assurance Engineering and Management,* vol. 10, no. 6, pp. 1527-1534, 2019.

[10] A. Moez, S. Mansour, C. Mohamed, and M. Driss, "Takagi-Sugeno Fuzzy Control of Induction Motor," *Proc. Int. Journal of Electrical and Electronics Engg,* vol. 2, no. 1, 2009.

[11] M. Allouche, M. Chaabane, M. Souissi, D. Mehdi, and F. Tadeo, "State feedback tracking control for indirect field-oriented induction motor using fuzzy approach," *International Journal of Automation and Computing,* vol. 10, no. 2, pp. 99-110, 2013.

General conclusion

This thesis has focused on the control of Permanent Magnet Synchronous Motors (PMSMs), which are increasingly used in industrial and automotive systems due to their high efficiency, compact size, and superior dynamic performance. However, PMSM drives are inherently nonlinear and sensitive to parameter variations and external disturbances, making their control a challenging task.

In Chapter 01, the mathematical modeling of the PMSM was presented, and its performance was analyzed under vector control strategies with and without inverter. These simulation studies highlighted the impact of inverter dynamics on system behavior and confirmed the need for robust and accurate control strategies.

In Chapter 02, the Mean Value Theorem (MVT) approach was investigated and applied to the PMSM. By transforming the nonlinear system into a Linear Parameter Varying (LPV) representation, the MVT framework facilitated the handling of nonlinearities. Simulation results confirmed the efficiency of this method in improving system response and robustness.

In Chapter 03, the design methodology of a PI–MVT–H_∞ controller was developed. This hybrid structure integrates the simplicity of PI control, the nonlinear system handling of the MVT method, and the robustness of H_∞ optimization. Although no simulation or experimental validation was carried out for this design, the theoretical formulation provides a solid foundation for future implementation of such a controller in PMSM drives.

Overall, this work established a clear path toward combining classical, nonlinear, and robust control techniques into a unified architecture suitable for PMSM applications. While the contributions remain primarily theoretical, they represent a significant step toward advanced robust control strategies for electrical drives.

Future Works

The work carried out in this thesis opens several perspectives for further research:

1. **Simulation of the PI–MVT–H∞ Controller:** Extending the work by implementing and simulating the designed controller on the PMSM model to evaluate its performance compared to conventional controllers.
2. **Experimental Validation:** Testing the controller on a real PMSM drive under different operating conditions, including load disturbances and parameter variations, to confirm its robustness and practical feasibility.
3. **Real-Time Implementation:** Developing digital implementations of the controller on DSP or FPGA platforms for applications such as electric vehicles and industrial automation.
4. **Adaptive and Intelligent Enhancements:** Integrating adaptation mechanisms or intelligent approaches (e.g., neural networks, fuzzy logic, reinforcement learning) to further improve robustness and adaptability.
5. **Broader Applications:** Extending the methodology to multi-machine systems, robotic manipulators, or renewable energy systems where PMSMs and robust control strategies are highly relevant.

By addressing these perspectives, the proposed PI–MVT–H∞ control approach could evolve from a theoretical framework into a practical and powerful solution for modern high-performance drive systems

Appendixes

1)- Appendix

Used values in the simulations results:

Parameter	Symbol	Value	Unit
Stator resistance	R_s	4.55	Ohm
Stator inductance	L_s	0.0116	Henry
Moment of inertia	J	7.36×10^{-4}	Kg.m^2
Permanent Magnets Flux	λ_{pm}	0.317	Wb
Friction Factor	f	6.11×10^{-5}	Nm/ Rad/ S
Pole Pair	p	02	Non unit
Power	P_n	1200	Watt